TECHNISCHE UNIVERSITÄT WIEN

Energy Economics Group

Master Thesis

for the achievement of the academic degree

Diplom-Ingenieurin

in the field of study Electrical Engineering
at TU Wien

Optimal Route Planning for Electric Vehicles with Special Consideration of the Topography

submitted at
Institute of Energy Systems and Electrical Drives

Supervisor: Priv.-Doz. Dipl.-Ing. Dr. Johann Auer
Assistent: Dipl-Ing. Andreas Fleischhacker, BSc

by

Theresia Perger
01125105

Vienna, May 2018

Acknowledgment - Danksagung

Besonderer Dank gilt meinen Betreuern Priv.-Doz. Dipl.-Ing. Dr. Johann Auer und Dipl.-Ing. Andreas Fleischhacker, BSc, für die gute Zusammenarbeit und ständige Unterstützung. Die Betreuung hat optimal funktioniert und sie standen mir bei inhaltlichen Fragen stets zur Verfügung.

Ich möchte auch meiner Familie herzlich danken. Meine Mutter Dagmar Perger unterstützte mich im Laufe des Studiums in jeder erdenklichen Weise, ebenso mein Vater, Dipl.-Ing. Dr. Andreas Perger. Ohne ihn wäre dieses Studium so nicht möglich gewesen. Meiner Schwester Mag. Dr. Katharina Perger danke ich dafür, mich stets motiviert und ermutigt zu haben.

Meine engsten Freunde waren mir während der Studienzeit eine besondere Stütze. Ausdrücklichen Dank hierbei an Berenice Konvicka, die mir stets mit Rat und Tat beistand. Ebenso danke ich Christoph Bohrnhofer für den stetigen Zuspruch.

Sehr dankbar bin ich für die tolle Erfahrung auf Erasmus am Politecnico di Milano. Viele Freundschaften, besonders die mit Jessica Kehrer, sind bis heute erhalten geblieben.

Außerdem möchte ich all jenen Freunden danken, die dieses Studium gemeinsam mit mir absolviert haben. Bei Laborübungen oder bei Prüfungsvorbereitungen haben wir uns gegenseitig unterstützt und motiviert.

Abstract

In contrast to conventional routing systems that determine the shortest distance or the fastest path to a destination, this thesis works on route planning specifically designed for electric vehicles by finding an energy-optimal solution. The first step is to find a model of the energy consumption of the vehicle including heating, air condition, and other additional loads. The street network is modeled as a network with nodes and weighted edges in order to apply a shortest path algorithm that finds the route with the smallest edge costs. A variation of the Bellman-Ford algorithm, the Yen algorithm, is modified such that battery constraints can be included. In this work a multi-objective optimization problem with three optimization variables is solved with the help of the modified Yen algorithm. The variables represent the energy consumption (the vehicle should reach the destination with the highest state of charge possible), the journey time, and the cyclic lifetime of the battery (minimizing the number of charging/discharging cycles by minimizing the amount of energy consumed or regenerated). The optimization problem assigns weights to each variable in order to put emphasis on one or the other. The route planning system is tested for the Wienerwald near Vienna, Austria, and for the city of San Francisco, California. It can be noticed that the topography has a strong influence on the energy consumption. Depending on the start and destination, the results are different depending on the weight of the optimization variable. Different weather conditions or using a different electric vehicle can change the results as well.

Kurzfassung

Im Gegensatz zu gewöhnlichen Routenplanungssystemen, die entweder die kürzeste Distanz oder die schnellste Route zum Ziel angeben, beschäftigt sich diese Diplomarbeit mit der Erarbeitung einer Routenplanung, die speziell für Elektrofahrzeuge konzipiert wird, um den energieeffizientesten Weg anzuzeigen. Im ersten Schritt wird ein Modell entwickelt, dass den Energieverbrauch des Elektrofahrzeuges inklusive Heizung, Klimaanlage und anderer zusätzlicher Verbraucher beschreibt. Das Straßennetzwerk wird als Netzwerk mit Knoten und gewichteten Kanten modelliert, um einen Algorithmus anzuwenden, der den Weg mit den geringsten Kosten findet. Eine Variation des Bellman-Ford Algorithmus, der Yen Algorithmus, wird so angepasst, dass Nebenbedingungen der Batterie miteinbezogen werden können. In dieser Arbeit wird eine Multi-Kriterien Optimierung mit drei Optimierungsvariablen mit Hilfe der modifizierten Version des Yen Algorithmus gelöst. Die Optimierungsvariablen stehen für den Energieverbrauch (das Fahrzeug soll mit dem hochstmöglichen Ladezustand am Ziel ankommen), die Reisedauer und die zyklische Lebensdauer der Batterie (die Anzahl an Lade-/Entladezyklen wird minimiert, indem der Betrag der verbrauchten beziehungsweise erzeugten Energie minimiert wird). Den Variablen werden Gewichte zugeordnet, damit diesen unterschiedliche Bedeutung im Optimierungsproblem zukommt. Die Routenplanung wird für den Wienerwald in Österreich und für San Francisco in Kalifornien getestet. Den Ergebnissen zufolge hat die Topographie der Streckenprofile einen starken Einfluss auf den Energieverbrauch. Je nach Start und Endpunkt der Reise fallen die Ergebnisse abhängig vom Gewicht der Optimierungsvariablen unterschiedlich aus. Außerdem verändern Wetter, Außentemperatur und Fahrzeugtyp die Ergebnisse.

Contents

1 Introduction

1.1 Motivation

Combustion engine driven cars have been dominating our world for more than a century. With global warming ahead and access to resources becoming more and more difficult, vehicles with electric motors could be part of the solution. They do not emit carbon dioxide or other emissions that could hurt humans or the environment, if the electrical power comes from renewable sources. Also, their overall efficiency is much higher than combustion engines. The ability to power vehicles with electrical engines is known for quite a long time. The question is why electric vehicles are not the majority already.

A lot of new problems come up with this new way of transportation. Despite using less energy, the task to store energy in the vehicle has been a difficult one. In the past years, the technology to use lithium ion batteries has improved. They became safer, more steady, and cheaper. Some producers of premium electric vehicles provide capacities of up to 100 kWh. With some more affordable models, capacities between 20 to 30 kWh are available. The range that comes with these capacities is not very easy to predict, but it can be said that this is the property of the vehicle which causes the most doubt in costumers. Starting with a fully charged battery, only a few hundred kilometers are within reach until the next charging event has to take place.

High energy consumption of fossil fuel powered vehicles is more of an economic problem or, for those who are concerned, an environmental problem. At gas stations the tank can be refilled within a few minutes and the car is good to go again for hundreds of kilometers. The owner of an electric vehicle faces other problems. Once the state of charge of the battery reaches the bottom, re-charging takes up a lot more time than refilling a tank.

Planning a trip with your vehicle becomes more difficult when traveling distances that could exceed the battery's range. A good advice would be to research the location of charging stations beforehand, and to plan the route wisely. Energy consumption can vary a lot depending on which path has been chosen. Clearly, it increases with increasing distance and velocity. But there are other impacts that show a different behavior than conventional cars. One of the major distinctions is the possibility to regenerate energy and charge the battery again while driving. This can happen while braking or driving downhill.

This thesis has the goal to find an optimal route to a desired destination while considering the special characteristics of electric vehicles. The main focus lies on energy consumption and the influence of the topography, as well as other properties like journey time and improving the battery lifetime.

1.2 Research Question and Method

The first main objective of this work is to find a route from a start to a destination point with the least amount of energy used. This task will be expanded, such that it is possible to get a route for the shortest journey time and one that should be the best to increase battery lifetime. Then those route planning options will be combined to a multi-objective optimization problem. Energy, time, and battery lifetime will be the optimization variables. Each variable will be weighted in order to put emphasis on one or the other.

The method is based on shortest path algorithms that use networks with nodes and edges, which have assigned values called edge costs. With the help of those algorithms, it is possible to find the path from one node to another node with the smallest edge costs (sum of the costs of all the edges on the path). The edge costs can have different meanings, for example the energy consumption on a section between two nodes. The nodes are the decision points of the network.

The edge costs of the energy consumption have to be approximated by a model of the electric vehicle. It includes the energy required for driving as well as additional loads for air condition and other accessories. It will be considered if the engine acts as a motor or as a generator in order to benefit from regenerative energy.

1.3 Structure of this Work

The following chapter, chapter 2, gives an overview on the work that has been done so far on this topic.

Chapter 3 starts with a flow chart in order to explain the problem and the solution that is proposed in this work. The model, which is used to calculate the vehicle's energy consumption, and the impact of additional loads and efficiencies on the vehicle are described. Also, the street network model is explained, and the last part is applying shortest path algorithms in order to see results for energy-optimal route planning, time-optimal route planning, and battery lifetime-optimal route planning as well as solutions for multi-criteria optimization.

Chapter 4 shows the results of the optimization algorithms with the chosen street networks, which are the Wienerwald area in the west of Vienna, Austria, and the city of San Francisco, California.

Then there will be a sensitivity analysis in chapter 5 comparing two different electric vehicles and different driving conditions. A comparison of the results of the different networks and scenarios is following.

Chapter 6 contains a conclusion and an outlook on future tasks on this topic.

2 State of the Art

2.1 Dynamic Optimization and Shortest Path Algorithms

Route planning is a dynamic optimization task, since every decision on where to continue on the path influences the next decisions. There is usually no standardized solution to those problems, but for route planning shortest path algorithms are widely used. Those algorithms work with networks that consist of nodes and edges with so-called edge costs. The goal is to find the path with the least amount of edge costs from one specific node to another.

Dijkstra's Shortest Path Algorithm

Dijkstra's algorithm is a very efficient method in order to find the shortest path between two nodes in a weighted graph network. Therefore it is widely used in network theory. The algorithm in detail can be found in (Dijkstra, 1959). It only works with positive edge costs, which is fine for shortest distance and shortest journey time optimization.

Bellman-Ford Algorithm

The Bellman-Ford algorithm (Bellman, 1958) can be used in networks with negative edge costs, which is an advantage compared to the Dijkstra algorithm. The disadvantage would be its higher complexity, which can be crucial in networks with a large number of nodes. If searching for an energy-optimal path, the edge costs represent the energy consumption of the electric vehicle. Energy can either be consumed or regenerated in case of an electric vehicle, therefore the costs can be positive and negative.

Yen Algorithm

The Yen algorithm (Yen, 1970) is an improved version of the Bellman-Ford algorithm. It has the same worst-case complexity, but generally finds the optimal path faster. It works

well with real-world street networks. In this work, the Yen algorithm was adapted and then applied to the route planning.

2.2 Route Planning for Electric Vehicles

In this section there will be a brief overview on the work that has already been done on optimal route planning for electric vehicles. Let's start with (Neaimeh et al., 2013), where it was pointed out that the a lot of people, who tested electric vehicles, experience so-called range anxiety. It turned out that because of this, many drivers would change their driving behavior and especially their choice, which route to take to the destination, if they are going on longer trips. Neaimeh et al. used a multiple linear regression model to include the topography information (the slope of the road) and predicted speed in their calculation of the energy consumption as well as data like efficiencies that are derived from previous journeys. In order to find an optimal route that can extend the range of the vehicle Dijkstra's shortest path algorithm was applied. The goal was not to simply find the energy-minimal route, but also to help with range anxiety and making drivers feel more comfortable with e-mobility.

Moving on to 'Energy-optimal driving range prediction for electric vehicles' (De Nunzio and Thibault, 2017). De Nunzio and Thibault created a range estimation for on-line use, which works by calculating the energy optimal route. The vehicle's energy consumption is modeled with influences of traffic conditions included. Then, with a shortest path algorithm, the Bellman-Ford algorithm, the range can be estimated. According to (De Nunzio and Thibault, 2017), it is more accurate than approximations using knowing only the distance to the destination or using the average energy consumption of the vehicle.

Martin Sachenbacher, Martin Leucker, Andreas Artmeier, and Julian Haselmayr worked on developing an energy-optimal routing system for electric vehicles in (Sachenbacher et al., 2011). In the paper an A* search is used and then compared to other shortest path algorithms performance-wise.

Another interesting work has been done by Sabine Storandt and Stefan Funke (Storandt and Funke, 2012). They include the possibility of battery switch station and use a modification of Dijkstra's algorithm. The modification is done by using Johnsons' shifting technique in order to include regenerated energy of the electric vehicle.

Battery switch stations did not establish, but charging stations for electric vehicles did and they are becoming more and more common. So in 'Enabling E-Mobility: One Way, Return, and with Loading Stations' (Storandt, Eisner, and Funke, 2013), the approach was similar to (Storandt and Funke, 2012), but including charging stations instead of battery switch stations. It was also proposed to work on a multi-criteria optimization that

includes the journey time and a maximum number of recharging events. For example, the travel time of the energy optimal path should not be more than 10% longer than the journey time of the shortest trip. Another option mentioned in (Storandt, Eisner, and Funke, 2013) would be bounded distance or bounded travel time.

This thesis will also include a multi-objective optimization in order to find a path that suits the driver's requirements best. The optimization will use weighting factors in order to put emphasis on these three optimization variables:

- Energy consumption: The user should reach the destination with the highest possible state of charge of the battery.
- Time: The journey time should be as short as possible.
- Battery lifetime: In order to increase the battery lifetime of the electric vehicle, the number of charging and discharging cycles should be as small as possible.

The goal here is to include the driver's preferences in a very flexible way. For example, the driver can choose a single-objective optimization minimizing the journey time, or giving equal weights to all three variables. Charging stations for electric vehicles are not included in this work.

3 Methodology

3.1 Flowchart

For the goal of this work - to find the optimal path to a desired destination with an electric vehicle - it is important to have a model describing the energy consumption of the electric vehicle, the journey time, and the street network. Then, shortest path algorithms can be used for optimization. Figure 3.1 shows a flow chart to give an overview of the problem.

We start by defining a start and a destination point. Then, it is necessary to have a road network that contains all possible paths between start and end point. It should also include topography information. Each road segment has a defined length s, a velocity v, which will be the speed limit in this case, and the slope q in %, calculated from the topography information.

The next step is to define the vehicle parameters. The initial state of charge of the battery SoC_{init} and its maximum capacity $SoC_{\max}$ are important to know, as well as the mass m, drag coefficient c_w and cross sectional area A of the vehicle (see section 3.2.1). The details considering the load of the accessories P_{acc} and the efficiencies η are explained in sections 3.2.3 and section 3.2.4, respectively.

When having information on the outside temperature, all parameters are ready for the calculation of the energy consumption of the electric vehicle and the journey times on all the road sections of the network.

As this work formulates an optimization problem with constraints, the boundary conditions have to be defined. Naturally, the state of charge of the battery SoC cannot be negative or above the maximum capacity. In the interest of the vehicle owner, the SoC should not fall below a certain minimum capacity, because a deep discharge can decrease battery lifetime. A factor a, $0 \leq a < 1$, is added to the optimization problem, such that the constraint equation becomes

$$a\, SoC_{\max} \leq SoC \leq SoC_{\max}. \tag{3.1}$$

The task will be extended to a multi-criteria optimization, with the variables energy, time, and battery lifetime. The factors γ and δ, with $\gamma + \delta \leq 1$, are used to give weights to the optimization variables. The last step is to apply a shortest path algorithm.

3.2 Modeling the Electric Vehicle

3.2.1 Calculation of the Energy Consumption on a Road Section

We start describing the model with the calculation of the energy consumption of an electric vehicle on a road section. When a vehicle is moved, certain forces act on the vehicle. Those are responsible for the amount of energy needed and they will be explained in detail in this section. The basic principles of the calculations are the same for both conventional as well as electric vehicles. The following parameters are necessary to use for the calculations:

m	mass of the EV	kg
g	gravitation constant	ms^{-2}
f_R	rolling resistance coefficient	
A	cross sectional area of EV	m^2
q	slope	%
α	slope	rad
c_w	drag coefficient	
ρ	air density	kgm^{-3}
v	velocity	ms^{-1}
a	acceleration	ms^{-2}
T	temperature	°C

Some of those parameters come from the vehicle itself, and others are road characteristics. Velocity and acceleration can also be influenced by the driving behavior, which is generally unknown. One way to include data on driving behavior would be using the ARTEMIS (Assessment and Reliability of Transport Emission Models and Inventory Systems) project, which is a large database of real world driving behavior of European drivers. For this work it was decided to use simplifications that exclude driving behavior.

Now, a road section with constant velocity, zero acceleration and constant slope is considered. We start by finding an approximation of the driving resistance F_{drive}, following (Haken, 2013). The total driving resistance consists of the rolling resistance, air resistance, and gradient resistance. Other parts, which are neglected in our calculation for simplification, come from acceleration, wind, and curves along the road. In the following parts, F_{drive} is explained in more detail.

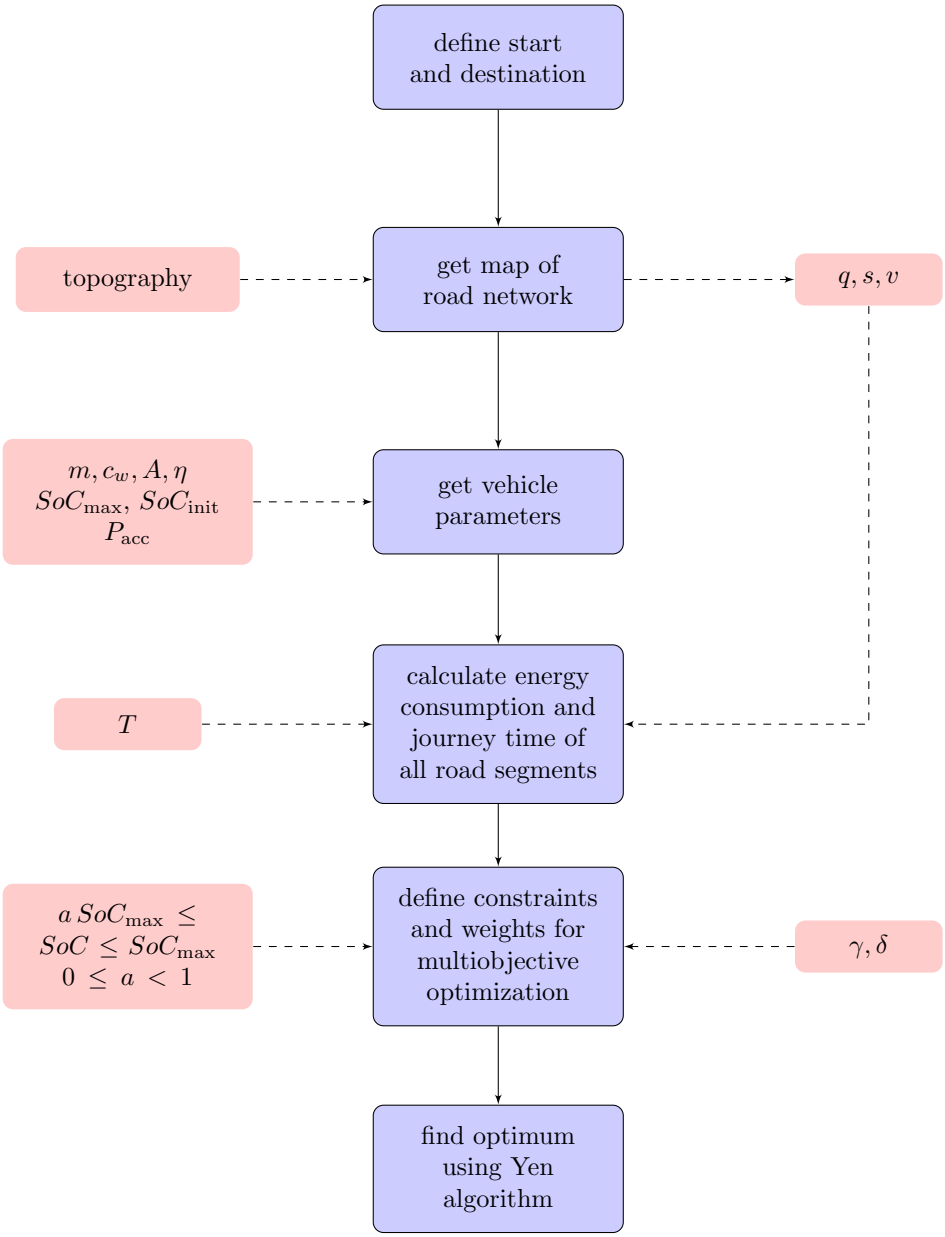

Figure 3.1: Flowchart of the optimization problem

Rolling Resistance

The rolling resistance of a vehicle is the primary force acting at low, constant speed. The tiers of a car are filled with gas and the mass of the vehicle deforms the wheel. This results in a force F_{roll}.

Following (Haken, 2013), the sum of the normal forces acting on each wheel is

$$\sum F_{\text{N}} = mg\cos(\alpha). \tag{3.2}$$

Because of the deformation, the rolling resistance coefficient f_R is introduced, leading to

$$F_{\text{roll}} = f_R mg\cos(\alpha). \tag{3.3}$$

In this approximation, f_R is considered a constant, although it can vary with temperature, internal pressure, speed and structure of the road. According to (Haken, 2013), it can go from 0.008 to 0.35 for different surfaces. A very low value of f_R is typical for smooth surfaces, a high one for driving on sand, snow, or on a field. Those extreme road conditions rarely occur and for most common roads f_R is around 0.01. Other effects that would be part of the rolling resistance are very small compared to f_R and are therefore neglected.

Air Resistance

The air resistance depends mainly on the velocity of the electric vehicle and the wind. In this work, the effects of any kind of wind are neglected. Local magnitude and direction of wind are hard to predict and change very quickly in time.

The following equation is widely used to calculate the air resistance without wind, see (Haken, 2013):

$$F_{\text{air}} = \frac{1}{2}\rho c_w A v^2. \tag{3.4}$$

In this equation there are some interesting variables. Let us consider the drag coefficient c_w, and the cross sectional area, A. Both are characteristics of the vehicle. They can be treated as constants for the optimization task of this work, but they can change if the same route is taken with a different vehicle. The area A is somewhere around $2\,\text{m}^2$, depending on the size and the type of the car. The average of the drag coefficient c_w in 2003 was 0.32, but has improved since then. In modern electric vehicles c_w can have values around 0.28. The parameter ρ is the air density. It changes with altitude, temperature, and humidity.

Gradient Resistance

Since the purpose of this work is to find an optimal route for electric vehicles while considering the influence of topography, this part of the driving force is key. The slope q of a road section is usually given in %. It is calculated dividing the rise by the run and multiply it by 100.

In order to get to the slope in radian, the conversion

$$\alpha = \operatorname{atan}(q/100) \tag{3.5}$$

has to be done. Knowing α and the mass of the vehicle m, the gradient resistance is calculated as

$$F_{\text{grad}} = mg\sin(\alpha), \tag{3.6}$$

according to (Haken, 2013). When there is zero slope, then $F_{\text{grad}} = 0$. When α is positive, energy is consumed by the vehicle. If F_{grad} is negative and can compensate the other parts of the driving force, then energy is generated.

Energy Consumption for Driving

The calculation of the total energy consumption for driving takes advantage of a few simplifications, such as constant velocity and slope, zero acceleration, no wind, and no curves on the path. The total driving force with our simplifications is

$$\begin{aligned} F_{\text{drive}} &= F_{\text{roll}} + F_{\text{air}} + F_{\text{grad}} && (3.7)\\ &= mgf_R\cos(\alpha) + \frac{1}{2}\rho c_w A v^2 + mg\sin(\alpha). && (3.8) \end{aligned}$$

In order to calculate the energy consumption, it is either possible to compute the integral of the driving force over the distance or the integral of the power over time. In general, it is practical to calculate the power resulting from the driving force from

$$P_{\text{drive}}(t) = F_{\text{drive}}(t) \cdot v(t). \tag{3.9}$$

Now we have the driving power P_{drive}, which we can add to other loads coming from accessories, such as heating, cooling and light (see section 3.2.3). The energy over a certain period $t_1 \leq t \leq t_2$ would be

$$E_{\text{drive}} = \int_{t_1}^{t_2} P_{\text{drive}}(t)\,\mathrm{d}t. \tag{3.10}$$

With the simplification of having constant velocity and constant F_{drive} over the time $t \in [t_1, t_2]$, we have

$$P_{\text{drive}} = F_{\text{drive}} \cdot v, \tag{3.11}$$

and then finally

$$E_{\text{drive}} = P_{\text{drive}} \, \Delta t, \tag{3.12}$$

with $\Delta t = t_2 - t_1$. If the total energy consumption from start to destination is needed, the values of all the sections just have to be added up.

3.2.2 Including Acceleration and Regenerative Braking

The previous section has shown how the model is approximating the energy consumption on a road section using the simplification of driving with constant velocity. The exact course of the acceleration is not known and depends a lot on the driver and road conditions. Therefore it was assumed that we have constant speed and zero acceleration on the road sections, but the change of the speed between two sections should be included as well. This is done by calculating the increase of kinetic energy between two sections.

The same goes for decreasing velocity between two sections. It is possible to receive the energy regenerated from braking, which only works in vehicles with electric motors. The energy that is necessary to accelerate or decelerate the vehicle to another speed level would be

$$E_{\text{kin}} = \frac{1}{2} m (v_{\text{next}}^2 - v_{\text{prev}}^2), \tag{3.13}$$

with m being the total mass of the vehicle including the passengers and baggage, v_{prev} the velocity of the current section of the road, and v_{next} the velocity of the following one. If v_{next} is higher than v_{prev}, it means that the battery must provide power for accelerating the vehicle. On the other hand, if v_{next} is lower than v_{prev}, the vehicle is braking and energy is fed back into the battery. The effects that efficiencies is explained in section 3.2.4.

It is important to note that this approach is a very basic one. The infinitely fast change in speed, which is assumed here, is physically not possible. Another option would be having a constant acceleration in order to have linear increasing (or decreasing) velocity until the next speed level is reached. When v in (3.8) is not a constant, but a linear function $v(t) = a \cdot t$, with a as the constant acceleration, (3.9) would contain $v^3(t)$, which makes the integral in (3.10) much more complex. It would also be quite vague to assume a certain acceleration, since this is very dependent on the driving behavior. For said reasons, the simplified approach is used in the calculations, but the effects of acceleration and braking are not neglected.

3.2.3 Including Accessory Loads

The energy that is used for moving the vehicle is not the only load decreasing the state of charge of the battery. Depending on the outside temperature, the passengers of the vehicle want heating or cooling. In case of conventional cars with internal combustion engines the waste heat is able to provide most of the energy the heating needs. Turning on air condition increases fuel consumption, but this is more of an economic problem rather than a question of decreasing range, since refueling is fast and easy.

For electric vehicles, where the battery is the only source of energy (apart from regenerative energy from braking or driving downhill), heating and cooling can influence the possible range tremendously - in a negative way. Other loads can be, for example headlights, fan, windshield wipers, rear window heating, and radio. The loads apart from driving are called 'accessories' in this work.

Actual measurements of the energy consumption of accessories can be found in (Geringer and Tober, 2012), where a lot of tests have been done on a few electric vehicles, including Nissan Leaf and Mitsubishi i-MiEV. Those two will serve as references in this work. It can be noticed that the power depends a lot on the type of electric vehicle. Independently of the model or brand, some generalizations can be made anyway.

For example, the radio and windshield wipers are not among the major loads. The wipers only need around 20 to 80 W and are turned on only when necessary. The radio consumes even less, only a few Watts. For the main task of this work, those two loads will be neglected in the calculations.

The dimmed headlights need between 50 W and 150 W. Depending on the country and road type, lights can be compulsory during daytime. Therefore they will be considered a steady load. High beam headlights on the other hand have a much higher consumption of a few hundred Watts. Since they are switched on only occasionally, there is no need to add them to the energy consumption of the accessories.

The consumption of the fans is included, because they are working constantly. Settings on 'medium' are assumed, because they are the most likely to be used. The power is usually between 40 and 100 W. Settings on 'very high' have a much higher demand (200 W or more).

The highest accessory loads would be heating and cooling, if they are needed. The reference values for the power vary a lot from model to model. They usually lie between 0.8 kW and 1.5 kW per 10 °C deviation, according to the measurements in (Geringer and Tober, 2012). Low temperatures, which need the heating to operate, are very common in many parts of the world. It can be a crucial factor on the range of the vehicle and influence the state of charge of the battery.

Table 3.1: Low voltage loads (Jeschke, 2016)

12 V load	typical values
Radio	20 W
Parking lights	8 W
Dimmed headlights	110 W
Windshield wipers	50 W
Instrument panel lights	22 W
License plate lights	30 W
Rear window heating	200 W
Braking lights	42 W
Fog lights	110 W
Rear fog lights	21 W
Turning signal	42 W

There is one essential difference between heating/cooling and the other loads. The battery of the electric vehicle is high voltage, while some loads need low voltage and therefore a DC-DC converter. Inside the vehicle there is a high and a low voltage network. The high voltage drives the engine as well as heating and cooling. The low voltage (12 V) typically provides the accessory loads in table 3.1, as in (Jeschke, 2016), and a 12 V battery, which is important for safety reasons. If the main battery fails, the 12 V network supplies braking and steering.

The overall power for the accessories that are considered in this work is

$$P_{\text{acc}} = P_{\text{hc}} + P_{\text{light}} + P_{\text{air}}, \tag{3.14}$$

with P_{hc} being the power needed for either heating or cooling, P_{light} the power for the dimmed headlights and P_{air} the power for the fan on medium setting. To calculate the energy demand over a certain period $t_1 \leq t \leq t_2$, the integral of the power P_{acc} over the time is used:

$$E_{\text{acc}} = \int_{t_1}^{t_2} P_{\text{acc}}(t)\,\mathrm{d}t. \tag{3.15}$$

3.2.4 Including Efficiencies

The overall tank-to-wheel efficiency of an electric vehicle is a lot better than the efficiency of a car with a combustion engine. This is one of the main advantages of electric vehicles, since less energy is necessary to move the car. On the other hand, the storage capacity is a lot smaller which can lead to problems with the range. The energy is stored in a

battery that has a charging efficiency η_{cha} and a discharging efficiency η_{dis}. Then there is a DC-AC inverter with an efficiency η_{inv}. The engine itself has the efficiency η_{m} when acting as a motor, or η_{g} as a generator. Other losses can occur at the final drive (η_{d}), the interface between vehicle and road. Since electric vehicles do not have a gear box, no gear box efficiencies are considered.

The accessories light, fan, radio, rear window heating, windshield wipers, and heating for the seats are low voltage loads. They need a DC-DC converter with an efficiency of η_{acc} because the battery is high voltage. Heating and cooling on the other hand operate on high voltage, without inverter, but with efficiency η_{hc}.

The next section 3.2.5 explains in more detail how those efficiencies influence the model of the electric vehicle. A summary of all the efficiencies that are considered in this work can be found in table 3.2.

Table 3.2: All efficiencies that are part of the calculation

Final drive	η_{d}
Motor	η_{m}
Generator	η_{g}
DC-AC inverter	η_{inv}
Accessories	η_{acc}
Heating and cooling	η_{hc}
Charging	η_{cha}
Discharging	η_{dis}

3.2.5 Energy Flow as a Motor or Generator

In the previous sections of this chapter it was explained how the energy consumption for driving and for the accessories is calculated. Now they need to be combined considering the efficiencies and the energy flow, which is described in this section.

Engine Operates as a Motor

When no energy is regenerated, the engine acts solely as a motor, which means that the battery is discharging. Figure 3.2 shows the corresponding energy flow from the battery to the accessories as well as the wheels. The graph shows which are the corresponding efficiencies η of the components battery, accessories, motor, and final drive. E_{out} is the energy taken from the battery, while E_{acc} and E_{hc} represent the energies which the

12 V-accessories and the heating and cooling units would need, respectively. E_{drive} is used for driving (see (3.9)).

The energy E_{out} that comes out of the battery has to supply the accessories, heating and cooling, and the final drive. It is calculated as

$$E_{\text{out}} = \frac{1}{\eta_{\text{d}}\eta_{\text{m}}\eta_{\text{inv}}} E_{\text{drive}} + \frac{1}{\eta_{\text{acc}}} E_{\text{acc}} + \frac{1}{\eta_{\text{hc}}} E_{\text{hc}}. \tag{3.16}$$

The actual energy that the battery is losing, considering the discharge efficiency, is

$$E = \frac{1}{\eta_{\text{dis}}} \left(\frac{1}{\eta_{\text{d}}\eta_{\text{m}}\eta_{\text{inv}}} E_{\text{drive}} + \frac{1}{\eta_{\text{acc}}} E_{\text{acc}} + \frac{1}{\eta_{\text{hc}}} E_{\text{hc}} \right) \tag{3.17}$$

$$= \frac{1}{\eta_{\text{dis}}} E_{\text{out}}. \tag{3.18}$$

The difference between E_{out} and E needs a brief explanation. E_{out} would be the energy that comes out of the battery and could be measured with a watt-meter. E on the other hand is only measurable indirectly by observing the state of charge of the battery. It is the total amount of energy the battery is giving away (motor-case) or receiving (generator-case).

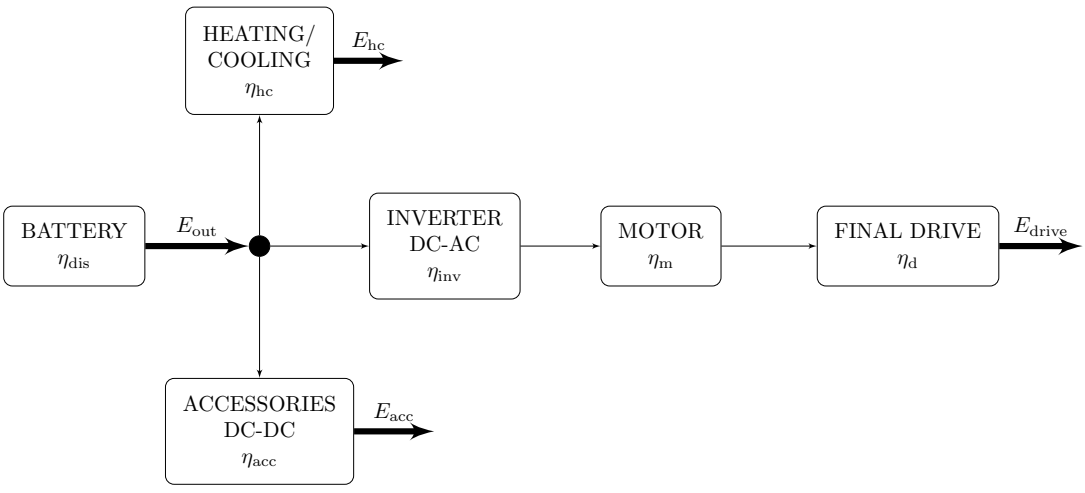

Figure 3.2: Energy flow-chart (motor)

Engine Operates as a Generator

When the engine acts as a generator, there is more variation. While energy is regenerated due to regenerative braking or driving downhill, the engine can provide energy for the battery and the accessories (see figure 3.3). There are two cases to distinguish. Depending on how much energy is gained by driving compared to what is consumed by the accessories:

1. **Discharging of the battery**: The energy that comes in (E_{regen}) feeds the accessories, but is not enough to cover the whole load E_{acc}. Therefore the battery needs to provide for the remaining energy and is discharging.
2. **Charging of the battery**: The regenerative energy is enough to cover all accessory loads E_{acc} and E_{hc}, and the rest can be used to charge the battery.

The energy $E_{\text{out}} = -E_{\text{in}}$ can be calculated as

$$E_{\text{out}} = -\eta_{\text{d}}\eta_{\text{g}}\eta_{\text{inv}}E_{\text{regen}} + \frac{1}{\eta_{\text{acc}}}E_{\text{acc}} + \frac{1}{\eta_{\text{hc}}}E_{\text{hc}}, \tag{3.19}$$

and the total energy that effects the state of charge of the battery is

$$E = \begin{cases} \frac{1}{\eta_{\text{dis}}}\, E_{\text{out}}, & \text{if } E_{\text{out}} > 0 \\ \eta_{\text{charge}}\, E_{\text{out}}, & \text{if } E_{\text{out}} < 0 \\ 0, & \text{if } E_{\text{out}} = 0. \end{cases} \tag{3.20}$$

This means that if E_{out} in (3.19) is positive, the state of charge (SoC) of the battery decreases, while when it is negative, the SoC is increasing.

If certain simplifications are possible, the motor- and the generator-case can be combined. If the efficiency of the engine working as a motor is the same as for a generator ($\eta_{\text{m}} = \eta_{\text{g}}$), equation (3.16) and (3.19) become

$$E_{\text{out}} = \left(\frac{1}{\eta_{\text{d}}\eta_{\text{m}}\eta_{\text{inv}}}\right)^{\text{sgn}(E_{\text{drive}})} E_{\text{drive}} + \frac{1}{\eta_{\text{acc}}}E_{\text{acc}} + \frac{1}{\eta_{\text{hc}}}E_{\text{hc}}. \tag{3.21}$$

If charging and discharging efficiency of the battery are equal ($\eta_{\text{cha}} = \eta_{\text{dis}}$), equation (3.18) and (3.20) merge to one new equation

$$E = \left(\frac{1}{\eta_{\text{dis}}}\right)^{\text{sgn}(E_{\text{out}})} E_{\text{out}}. \tag{3.22}$$

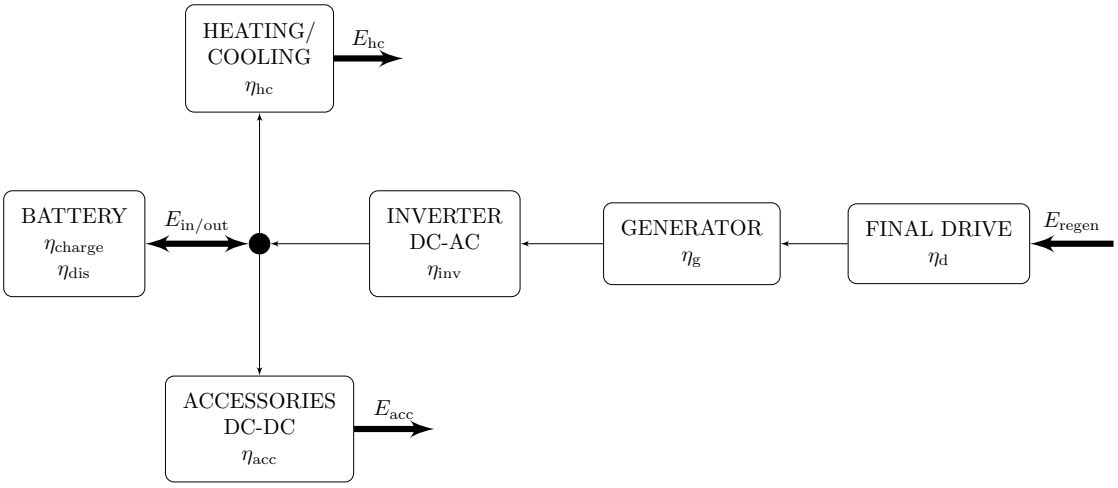

Figure 3.3: Energy flow-chart (generator)

3.2.6 Calculation of the Total Energy between Two Points

The preceding sections explain how the energy of a road section is calculated according to the proposed model. It includes the consumption for the purpose of driving, the loads of the accessories and the efficiencies.

Usually, the road connecting two points has varying properties along the way. In this model, the slope and the maximum speed can change, while the road conditions, outside temperature, mass of the vehicle, and other properties are constant.

Let's say over a distance of s_i, there is a slope of α_i and a velocity of v_i, both being constants. The following section has a length s_{i+1}, a slope of α_{i+1} and a velocity of v_{i+1}. The road that connects two points can be split up in N segments, such that the energy consumption of segment $i \in I = (1, \ldots, N)$ would be

$$E_{\mathrm{out},i} = \left(\frac{1}{\eta_{\mathrm{d}}\eta_{\mathrm{m}}\eta_{\mathrm{inv}}}\right)^{\mathrm{sgn}(F(\alpha_i,v_i))} F(\alpha_i, v_i)s_i + \frac{1}{\eta_{\mathrm{acc}}}P_{\mathrm{acc}}t_i + \frac{1}{\eta_{\mathrm{hc}}}P_{\mathrm{hc}}t_i, \tag{3.23}$$

with F according to (3.8) and $t_i = s_i/v_i$. The change of kinetic energy between the sections i and $i+1$ would be

$$E_{\mathrm{kin},i} = \frac{1}{2}m(v_{\mathrm{i+1}}^2 - v_{\mathrm{i}}^2), \tag{3.24}$$

according to (3.13). On the road made of N segments, the electric vehicle would have a total energy consumption of

$$E = \sum_{i=1}^{N} \left(\frac{1}{\eta_{\text{dis}}}\right)^{\text{sgn}(E_{\text{out},i})} \left(\left(\frac{1}{\eta_{\text{d}}\eta_{\text{m}}\eta_{\text{inv}}}\right)^{\text{sgn}(F(\alpha_i,v_i))} F(\alpha_i, v_i)s_i + \frac{1}{\eta_{\text{acc}}} P_{\text{acc}} t_i + \frac{1}{\eta_{\text{hc}}} P_{\text{hc}} t_i \right) \tag{3.25}$$

$$+ \sum_{i=0}^{N} \left(\frac{1}{\eta_{\text{d}}\eta_{\text{m}}\eta_{\text{inv}}\eta_{\text{dis}}}\right)^{\text{sgn}(E_{\text{kin},i})} \frac{1}{2} m(v_{\text{i+1}}^2 - v_{\text{i}}^2). \tag{3.26}$$

3.3 Modeling the Street Network

The next task of the route planning is to model the real-life street network with all its properties such as slope, distances, speed limits, and road type. The route planning will require a shortest path problem to be solved. The existing shortest path algorithms need a specific structure of the network.

3.3.1 Networks

Different kinds of networks are usually made of nodes and edges. The nodes are connected with each other by edges, which can have assigned values. They are referred to as 'edge weights' or 'edge costs'. A network consisting of nodes and edges is also called 'graph'. A graph can be undirected, unidirectional, or bidirectional. In the following paragraphs it is explained what nodes, edges, and edge costs mean in this context.

Nodes

Nodes are the decision points of the network. Each node is connected to different nodes via edges. Some nodes are directly connected, others are only reachable by passing other nodes on the way. In the real-world street network, nodes would be intersections of roads.

Edges

Edges are the roads connecting the nodes. Each edge starts with a node and ends with another node. In this network model, the edges are split into sections. Those sections are all straight, have constant slope, and a constant speed limit.

Edge costs

Networks have the purpose to express relations between the nodes. There are different ways to characterize those relations. The most simple one would be binary relations, which means that the only information is if there is a connection (an edge) or not. Edges can also have assigned values, the so-called edge weights or edge costs. They can have physical meanings like distances, or something more abstract like a value to express the strength of a relation between people in social networks.

It was briefly mentioned in the beginning of this section that a graph can have different forms of directiveness.

- Undirected graph: The edge cost is the same for going from node A to node B as it is for the other way.
- Unidirectional graph: There is only one way possible, from node A to B, but not from B to A.
- Bidirectional graph: The edge costs can be different going one way or the other.

An algorithm to find the shortest path would find the path that cumulates the least amount of edge costs on its way. When the edge costs have the physical meaning of energy consumption of an electric vehicle, we have a bidirectional graph. The main reason for this is the topography, because two nodes can be on a different height level and therefore the required energy is different for both directions.

3.3.2 Topography Data

For the information on topography, data was obtained from the 'USGS Earth Explorer' website, where a lot of geographical data is available for download. A digital elevation map coming from the NASA Shuttle Radar Topography Mission (SRTM) was taken from this website. It has a pretty high spatial resolution of one arc-second for longitude (east-west) as well as for latitude (north-south). The height resolution is one meter. The file obtained from USGS was a TIFF-file with 3601×3601 pixel.

Since two adjacent pixels are one arc-second apart, the TIFF-file covers an area of one degree in longitude and one degree in latitude. The testing of this method will be done for the area around Vienna, Austria. Therefore, the file provides topography information from 16°E to 17°E and from 48°N to 49°N.

For the calculations of the energy consumption of the electric vehicle, it is necessary to convert the distances in degrees into distances in meters. The conversion was done by an approximation of the earth as a perfect sphere with the radius of $R_{\text{earth}} = 6371\,\text{km} = 6371000\,\text{m}$. ϕ_1 and ψ_1 are the coordinates of a point in degree longitude and degree

latitude, respectively. ϕ_2 and ψ_2 are the coordinates of another point, and $\Delta\phi = \phi_1 - \phi_2$ and $\Delta\psi = \psi_1 - \psi_2$ are the distances between point 1 and point 2 (in degree). For the distances Δx for longitude and Δy for latitude in meters, we convert using

$$\Delta y = \frac{2\pi R_{\text{earth}}}{360}\,\Delta\psi, \tag{3.27}$$

and

$$\Delta x = \frac{2\pi R_{\text{earth}}}{360}\cos(\psi_1\pi/180)\,\Delta\phi. \tag{3.28}$$

It can be noticed that (3.28) does depend on the coordinates of the latitude. At the equator, both equations would be the same. The coordinate lines of the longitude come closer together when moving further away from the equator. Two places with a $\Delta\phi$ of 1° at the equatorial line have a much larger Δx than two places with the same $\Delta\phi$ at another degree of latitude. Considering Vienna again, the factor resulting from the cosine in (3.28) would be around 0.67. The resolution of one arc-second of the map obtained from NASA means having a resolution of about 31 m north-south, and a resolution of 22 m east-west in Austria. It has to be noticed that (3.27) and (3.28) are only approximations of the true distances.

The next task is to calculate the slope of a road section. A section, or road segment, is part of an edge as mentioned above. It is straight and has a constant gradient. The height difference Δz between the start and the end point of the segment is divided by the euclidean distance between those points and multiplied by 100 in order to get the slope q in %:

$$q = 100\,\frac{\Delta z}{\sqrt{(\Delta x)^2 + (\Delta y)^2}}. \tag{3.29}$$

The height data is derived from the TIFF-file mentioned in the beginning of this section.

3.3.3 Streets and Roads

In section 3.3.2 it was explained how topography data can be obtained. The next step is to get an adequate network of roads that contains the region of interest. For this task there are multiple options. One of them is using 'OpenStreetMaps', which is a big database for streets, roads, and paths. It also includes foot ways, water ways, and other paths cars cannot use. This turned out to be a problem for the area chosen for testing. Even though paths have labels, a major part of them is labeled 'unclassified' or has an empty label. This was true even for main streets. It was nearly impossible to distinguish road types and filter out those which are useful in this work. The same goes for a lot of data derived from official governmental websites.

For those reasons, a more simple approach was chosen. First, it was decided which roads (edges) should be part of the network. Only the main roads of the 'Wienerwald' area in the west of Vienna were included. The nodes of the network are the intersections of these roads.

Some of the roads (edges) are a few kilometers long. They are split up in consecutive sections, which are straight and a few hundred meter long, making the roads polygonal chains. It should be discussed if it is more practical to use shorter sections because they have a higher resolution. Undoubtedly, the results would be more precise, but for the purpose of testing the proposed method and algorithm, this kind of precision is not necessary. On the other hand, if this method were to be used in an advanced route planning system, the network would have to be more precise.

The coordinates of the start and end points of the road segments and the matching topography information were obtained, and the distances and height differences were calculated as explained in section 3.3.2. This ensure each segment is straight and has a constant slope. The last missing piece of road information is the velocity. As explained in section 3.2.2, the velocity of each segment considered to be constant, it can only change between sections. To keep it simple, the legal maximum speed of each road segment was set to be the velocity of the vehicle.

3.4 Optimization

In this section it will be explained how the optimization algorithms are implemented in order to find the optimal path for an electric vehicle. The Bellman-Ford algorithm as well as its improved version, the Yen algorithm, are introduced. Then, the methods of path optimization for three different scenarios are described: finding the optimum in terms of energy consumption and time, as well as for battery lifetime. Those three variables are combined later on for multi-objective optimization.

3.4.1 Shortest Path Algorithms

Bellman-Ford Algorithm

Let's imagine a road network with N nodes that are connected with each other by edges with edge costs. The numbers assigned to the nodes are random, so we decide that the start point is node 1 and the destination is node N. Now f_i is the total costs required to travel from node i to node N, with $i = 1, 2, \ldots, N-1$ and $f_N = 0$. The algorithm in

detail can be found in (Bellman, 1958). It starts with the initial values $f_i^{(0)}$, and then continues iteratively with the index k:

$$f_i^{(k+1)} = \min_{j \neq i}(d_{ij} + f_j^{(k)}), \tag{3.30}$$

$$f_N^{(k+1)} = 0, \tag{3.31}$$

with d_{ij} being the costs of the edge connecting node i and j. Bellman chooses $f_i^{(0)}$ to be the costs from node i directly to N without passing any other node, such that

$$f_i^{(0)} = d_{iN}. \tag{3.32}$$

Now it becomes clear why the algorithm uses this kind of iterations. Iteration $k = 0$ gives the costs from each node to N with zero stops in between. The next step takes all combinations that go from i to N with a maximum of one stop between and compares them in order to find the path with minimum costs. The optimization for this iteration is

$$f_i^{(1)} = \min_{j \neq i}(d_{ij} + f_j^{(0)}), \tag{3.33}$$

$$f_N^{(1)} = 0, \tag{3.34}$$

which satisfy the inequality

$$f_i^{(1)} \leq f_i^{(0)}. \tag{3.35}$$

Then the iterative process goes on with k being the maximum number of stops between the nodes i and N. The optimal solution of each iteration converges to the absolute minimum f_i,

$$\lim_{k \to \infty} f_i^{(k)} = f_i. \tag{3.36}$$

After at most N iterations, the minimum to be found. Else, a negative loop exists in the network, not leading to any solution of the Bellman-Ford algorithm. The search for a minimum would continue forever.

In this work, the edge costs represent either time or energy consumption. Since any journey time between two nodes can only have a positive value, no negative loop is possible when travel time is optimized. For energy consumption, edge costs can have negative values because we are considering electric vehicles, which have the ability to act as a generators and charge their batteries under certain conditions. Yet negative loops do not occur in real-world street networks. It is physically impossible to gain energy when start and end point are the same. The only case where this could happen is when the electric vehicle is charged on its way, meaning some sort of energy source has been added to the problem.

Yen Algorithm

The Bellman-Ford algorithm has a relatively high order of complexity $\mathcal{O}(NM)$, with the number of nodes, N, and M, the number of edges of the graph. The Dijkstra algorithm would have a lower complexity, but cannot deal with negative edge costs. Therefore, it was searched for a solution to speed up the process.

The Yen algorithm, see (Yen, 1970), is an improved version of the Bellman-Ford algorithm. It usually finds the minimum faster than Bellman-Ford, and yet, in the worst-case scenario, it could take just as much time to compute. In this work, the optimization algorithms are based on Yen.

The algorithm uses the same principles as Bellman-Ford, searching the minimum costs from node $i = 1, 2, \ldots, N-1$ to node N for each iteration k. We set

$$f_i^{(0)} = d_{iN} \tag{3.37}$$

and proceed as follows. For odd values of k, the minimum has to be found using

$$f_i^{(2k-1)} = \min_{N \geq j > i} (d_{ij} + f_j^{(2k-1)}, f_i^{(2k-2)}), \tag{3.38}$$

$$f_N^{(2k-1)} = f_N^{(2k-2)}, \tag{3.39}$$

with $i = N-1, N-2, \ldots, 1$. For even values of k the minimizations is

$$f_i^{(2k)} = \min_{1 \leq j < i} (d_{ij} + f_j^{(2k)}, f_i^{(2k-1)}), \tag{3.40}$$

$$f_1^{(2k)} = f_1^{(2k-1)}, \tag{3.41}$$

with $i = 2, 3, \ldots, N$. The advantage of the Yen algorithm is clear now. For each iteration k not only the results from the previous iterations $k-1, k-2, \ldots, 0$ are used, but also those already computed in the k^{th}-iteration. Yen's version of the algorithm calculates more combinations during one iteration than Bellman-Ford, because it does not restrict to a maximum number of nodes (stops) on the path. This helps getting the optimized path sequences faster. If iteration k fulfills the condition

$$\boldsymbol{f}^{(k)} = \begin{bmatrix} f_1^{(k)} \\ f_2^{(k)} \\ \vdots \\ f_N^{(k)} \end{bmatrix} \equiv \begin{bmatrix} f_1^{(k-1)} \\ f_2^{(k-1)} \\ \vdots \\ f_N^{(k-1)} \end{bmatrix} = \boldsymbol{f}^{(k-1)}, \tag{3.42}$$

the algorithm has found the optimum.

3.4.2 Energy-optimal Route Planning

The search for an energy-optimal path in a network can be viewed as a shortest path problem. Using the Yen algorithm seems like an adequate approach. How it is applied in order to find the energy-optimal path is explained in this part.

In section 3.3 the structure of the network was described and in section 3.2 the calculation of the energy consumption was explained. If the optimization problem were without constraints, the Yen algorithm could be applied straightforward. Naturally, there are some boundaries to the problem coming from the battery. The state of charge (SoC) of the battery cannot exceed the following limits:

I. $SoC \leq SoC_{\max}$
   The state of charge cannot be higher than the maximum capacity of the battery $SoC_{\max}$. This is only relevant during driving in the case of regenerating energy by braking or going down-hill with the vehicle.
II. $SoC \geq a\, SoC_{\max}$, $0 \leq a < 1$
   The state of charge cannot be negative, once it is zero there is no more energy to obtain. Deep cycles are not beneficial to the battery, therefore the factor a is introduced. It limits the possible depth of discharge (DoD). Its value will be set reasonably, for example $a = 0.2$. This means that the DoD can be as low as 20% of the battery's full capacity. Including this kind of protection factor in the algorithm extends the battery's lifespan.

The Yen algorithm, as proposed by Jin Y. Yen in (Yen, 1970), as well as the Bellman-Ford algorithm, find the shortest paths from each node of the network to one specific node (compare section 3.4.1). The search goes backwards, always starting from the destination node, see (3.37). Let's go into detail what happens during a iteration. First, $f_i^{(k)}$ is decided according to the least costs from node i to the destination, node N. If this result is used to find the path from j to N, then d_{ji}, the costs from j to i, are added to the path. Since this path starts with d_{ji}, the state of charge at node i is a different one than it was assumed when deciding $f_i^{(k)}$, where the journey starts at i. It can happen that $f_i^{(k)}$ is not an optimal solution for the path from j to N. The whole algorithm is based on the assumption that the solutions found in the previous steps are indeed optimal. The state of charge (SoC) is always calculated forward, while the algorithm works backwards. This is not only a problem with finding the optimal path, but also with violating constraints.

The backwards iterations of the Yen algorithm are therefore not suitable for the optimization problem with the SoC-constraints. Therefore, the following solution was introduced. Instead of computing all minimum paths *to the destination*, all minimum paths *from the start* are calculated. Both ways the path of interest - from the start node to the destination node - is evaluated. The principles of the Yen algorithm remain the same,

there are a few modifications. f_i are now the costs from node 1, the start node, to node i.

We start with iteration 0

$$f_i^{(0)} = d_{1i}, \tag{3.43}$$

where d_{1i} are the edges from node 1 to node $i = 2, \ldots, N$. For odd iterations, the minimum is found using

$$f_i^{(2k-1)} = \min_{1 \leq j < i} (f_j^{(2k-1)} + d_{ji}, f_i^{(2k-2)}), \tag{3.44}$$

$$f_1^{(2k-1)} = f_1^{(2k-2)}, \tag{3.45}$$

with $i = 2, 3, \ldots, N$. For even iterations, the minimization is

$$f_i^{(2k)} = \min_{N \geq j > i} (f_j^{(2k)} + d_{ji}, f_i^{(2k-1)}), \tag{3.46}$$

$$f_N^{(2k)} = f_N^{(2k-1)}, \tag{3.47}$$

with $i = N-1, N-1, \ldots, 2$. For all iterations and steps, the constraints are checked. For the first constraint ($SoC \leq SoC_{\max}$), the path is still feasible if the constraint is violated, but the state of charge is set to the maximum capacity of the battery ($SoC = SoC_{\max}$), because no further charging is possible. The energy consumption $f_j^{(k)} + d_{ji}$ is adapted accordingly.

If the second constraint is violated ($SoC \geq a\, SoC_{\max}$), the specific path is considered unfeasible. If even the resulting minimum of (3.44) or (3.46) is unfeasible, $f_i^{(k)}$ is set to infinity. This path will be neglected by all further calculations. The constraints are checked for *all* road segments which are part of the edges. If the state of charge exceeds the lower limit in the middle of an edge, the whole edge is unfeasible.

Again, if all minimum paths remain the same compared to the previous iteration, the optimum is found:

$$\boldsymbol{f}^{(k)} = \begin{bmatrix} f_1^{(k)} \\ f_2^{(k)} \\ \vdots \\ f_N^{(k)} \end{bmatrix} \equiv \begin{bmatrix} f_1^{(k-1)} \\ f_2^{(k-1)} \\ \vdots \\ f_N^{(k-1)} \end{bmatrix} = \boldsymbol{f}^{(k-1)}. \tag{3.48}$$

3.4.3 Time-optimal Route Planning

Compared to the search for an energy-optimal path, finding a time-optimal one is a lot less complicated. On one hand, there are no constraints assumed concerning the

journey time. It is just about finding the fastest itinerary. On the other hand, there are no negative edge costs. In fact, the graph is undirected if it is assumed that the same road with the same speed limit is available for the way back.

This optimization problem could be solved with a less complex and faster algorithm than Bellman-Ford or Yen, because there are no negative edge costs. Although, when energy and time are combined to multi-objective optimization, it is easier to just use the same algorithm, because the computation time is not crucial in this work. The procedure is the same as for finding an energy-optimal path. The edge costs are representing the journey time in this case. For any road segment they are calculated as

$$t = v/s, \tag{3.49}$$

with the assigned speed level v and the length s of the section. The journey time of a whole edge connecting the nodes i and j is the sum of all M road segments:

$$t_{ij} = \sum_{l=1}^{M} t_l. \tag{3.50}$$

We start with iteration 0

$$g_i^{(0)} = t_{1i}, \tag{3.51}$$

where t_{1i} are the edges costs from node 1 to node $i = 2, \ldots, N$. For odd iterations, the minimum is found using

$$g_i^{(2k-1)} = \min_{1 \leq j < i} (g_j^{(2k-1)} + t_{ji}, g_i^{(2k-2)}), \tag{3.52}$$

$$g_1^{(2k-1)} = g_1^{(2k-2)}, \tag{3.53}$$

with $i = 2, 3, \ldots, N$. For even iterations, the minimization is

$$g_i^{(2k)} = \min_{N \geq j > i} (g_j^{(2k)} + t_{ji}, g_i^{(2k-1)}), \tag{3.54}$$

$$g_N^{(2k)} = g_N^{(2k-1)}, \tag{3.55}$$

with $i = N-1, N-1, \ldots, 2$.

3.4.4 Energy-optimal Route Planning in Order to Increase Battery Lifetime

There is also a third criterion that can be used for the route planning, which is the increasing of battery lifetime. Battery wear-off is something that should be avoided as

long as possible. It can decrease the capacity and limit the range of the vehicle. The battery is also a very expensive part of the electric vehicle to replace.

There are some actions the user of the vehicle could take in order to increase the battery's lifetime. First, avoiding deep discharge is helpful. This can be included in the factor a, which has been introduced in section 3.4.2. Tuning a to a value that is safe for the battery can do the job.

A lithium-ion battery, which is the power source for most electric vehicles, usually has a specific cyclic lifetime. Decreasing the number of cycles the battery has to go through helps it to stay alive longer. This is the third criterion of the multi-objective optimization. It works similar to the energy-optimal planning, but takes the absolute value of the energy as the edge costs. The power provided by the battery for driving or for the accessories is treated the same as regenerated energy from braking and driving downhill, which is now increasing the costs instead of decreasing them. The edge costs from node i to j is a_{ij}, and is the sum of the absolute energy values of all road sections belonging to this edge. h_i are the costs from node 1 to node i.

We start with iteration 0

$$h_i^{(0)} = a_{1i}, \tag{3.56}$$

where a_{1i} are the edges costs from node 1 to node $i = 2, \ldots, N$. For odd iterations, the minimum is found using

$$h_i^{(2k-1)} = \min_{1 \leq j < i} (h_j^{(2k-1)} + a_{ji}, h_i^{(2k-2)}), \tag{3.57}$$

$$h_1^{(2k-1)} = h_1^{(2k-2)}, \tag{3.58}$$

with $i = 2, 3, \ldots, N$. For even iterations, the minimization is

$$h_i^{(2k)} = \min_{N \geq j > i} (h_j^{(2k)} + a_{ji}, h_i^{(2k-1)}), \tag{3.59}$$

$$h_N^{(2k)} = h_N^{(2k-1)}, \tag{3.60}$$

with $i = N-1, N-1, \ldots, 2$.

3.4.5 Multi-objective Route Planning

The multi-objective optimization has three optimization variables: energy consumption of the vehicle, journey time, and cyclic lifetime of the battery. The algorithm applied for this task is still based on the modified version of the Yen algorithm from section 3.4.2. The shortest path from the start node number 1 to all nodes i is calculated in each iteration, taking into account the three variables and their weights.

We start with iteration 0 as usual, for all three variables in the same manner:

$$f_i^{(0)} = d_{1i}, \tag{3.61}$$

$$g_i^{(0)} = t_{1i}, \tag{3.62}$$

$$h_i^{(0)} = a_{1i}. \tag{3.63}$$

The next step is to go into the details of the odd iterations. At first,

$$f_1^{(2k-1)} = f_1^{(2k-2)}, \tag{3.64}$$

$$g_1^{(2k-1)} = g_1^{(2k-2)}, \tag{3.65}$$

$$h_1^{(2k-1)} = h_1^{(2k-2)} \tag{3.66}$$

are set. Then, for the other nodes i, the energy optimal path is calculated following (3.44) and $E_{min} = |f_i^{(2k-1)}|$ is set. The SoC-constraints are checked as explained in section 3.4.2. If at least one path is feasible, then T_{min} and A_{min} are calculated according to (3.52) and (3.57), respectively.

Now all three results are combined to multi-objective optimization with the weights γ for energy, δ for time, and $1-(\gamma+\delta)$ for battery lifetime. The optimization problem solved for node $i = 2, 3, \ldots, N$ in iteration $2k-1$ would be:

$$x_i^{(2k-1)} = \min_{1\le j<i} \Bigg(\gamma \frac{f_j^{(2k-1)} + d_{ji}}{E_{min}} + \delta \frac{g_j^{(2k-1)} + t_{ji}}{T_{min}} + (1-(\gamma+\delta)) \frac{h_j^{(2k-1)} + a_{ji}}{A_{min}}, \tag{3.67}$$

$$\gamma \frac{f_j^{(2k-2)}}{E_{min}} + \delta \frac{g_j^{(2k-2)}}{T_{min}} + (1-(\gamma+\delta)) \frac{h_j^{(2k-2)}}{A_{min}} \Bigg). \tag{3.68}$$

All energy costs are normalized by the factor E_{min}, the journey time by T_{min}, and the absolute energy by A_{min}. The normalized values are one for the optimum and greater one for all the other paths. The deviation from the optimum is then weighed by γ, δ and $1-(\gamma+\delta)$. After the minimum is found, the costs $f_i^{(2k-1)}$, $g_i^{(2k-1)}$, and $h_i^{(2k-1)}$ are set according to the resulting optimal path.

For even iterations the situation is very similar. We start with

$$f_N^{(2k)} = f_N^{(2k-1)}, \tag{3.69}$$

$$g_N^{(2k)} = g_N^{(2k-1)}, \tag{3.70}$$

$$h_N^{(2k)} = h_N^{(2k-1)}. \tag{3.71}$$

Then, for node i the optimal values E_{min}, T_{min}, and A_{min} are computed and multi-objective optimization is done:

$$x_i^{(2k)} = \min_{N \geq j > i} \Bigg(\gamma \frac{f_j^{(2k)} + d_{ji}}{E_{min}} + \delta \frac{g_j^{(2k)} + t_{ji}}{T_{min}} + (1 - (\gamma + \delta)) \frac{h_j^{(2k)} + a_{ji}}{A_{min}}, \tag{3.72}$$

$$\gamma \frac{f_j^{(2k-1)}}{E_{min}} + \delta \frac{g_j^{(2k-1)}}{T_{min}} + (1 - (\gamma + \delta)) \frac{h_j^{(2k-1)}}{A_{min}} \Bigg). \tag{3.73}$$

It has to be noted that those steps start with $i = N - 1$ and end with $i = 2$.

3.5 Reference Values and Assumptions

The calculations of the previous sections need actual values for the parameters and variables. We start with those which are independent of the vehicle (see table 3.3). The

Table 3.3: Values of the parameters independent of the vehicle

Constants			
Gravitational constant	g	9.81	ms^{-2}
Rolling resistance coefficient	f_R	0.01	-
Air density	ρ	1.2	kgm^{-3}

gravitational constant g is treated as a constant in this work, because the variations with altitude are very little on earth. The rolling resistance is $f_R = 0.01$, according to (Haken, 2013). It means that the conditions on all roads are assumed to be the same. The air density changes with altitude and weather conditions, but is considered to be a constant for simplicity as well.

The two vehicles picked out for the testing are the Nissan Leaf, see data sheet (Nissan, 2018), and the Mitsubishi i-MiEV, see data sheet (Mitsubishi, 2018). All parameters that are necessary in the calculations are summarized in table 3.5. For the mass m, the curb weight of the vehicle and the weight of one person, the driver, are combined. The driver's mass is assumed to be 75 kg, a pretty average value.

For the air resistance, the cross sectional area A, and the drag coefficient c_w are necessary according to (3.4). If A is not specified in the official data sheet, it is possible to estimate according to (Haken, 2013), knowing the width w and height h of the vehicle:

$$A = 0.81 \cdot w \cdot h. \tag{3.74}$$

In (Geringer and Tober, 2012) there is a lot of data available from the measurements on these vehicles. The measurements include the total energy consumption for various driving scenarios, power consumption of the accessories as well as heating and air condition, and measurements of the efficiencies of converters, battery, et cetera.

The power consumption of the accessories is also obtained from (Geringer and Tober, 2012). The power of the dimmed headlights of the Nissan Leaf is $P_{\text{light}} = 48\,\text{W}$. The Mitsubishi i-MiEV has a $P_{\text{light}} = 127\,\text{W}$, but it has the option of a daytime light with only 38 W. For the fans there are a few options. The power P_{air} of the Nissan Leaf is set to 62 W, which corresponds to setting 2, in the middle of the available range. The Mitsubishi has a total of eight settings. Setting number 2 with 48 W seemed like a reasonable choice, because high settings are turned on only occasionally.

The power needed for heating and cooling is a lot higher (see table 3.4). In order to make calculations easier, the power consumption was linearized. At 20 °C there is no need for either heating or cooling. Therefore, the power P_{hc} depends on the deviation of T from $T_0 = 20°\text{C}$:

$$P_{\text{hc}} = \begin{cases} P_{\text{cool}}(T - T_0), & \text{if } T > T_0 \\ P_{\text{heat}}(T_0 - T), & \text{if } T < T_0 \\ 0, & \text{if } T = T_0. \end{cases} \tag{3.75}$$

Table 3.4: Power consumption of the heating and cooling systems of Nissan Leaf and Mitsubishi i-MiEV from (Geringer and Tober, 2012)

Outside temperature	Nissan	Mitsubishi
30 °C	0.4 kW	0.3 kW
20 °C	0.0 kW	0.0 kW
10 °C	0.9 kW	1.0 kW
0 °C	1.9 kW	2.5 kW
−10 °C	2.8 kW	3.1 kW
−20 °C	2.7 kW	3.8 kW

Moving on to the efficiencies, there are no measurements of the final drive η_{d} and the motor η_{m}, which means they have to be assumed. For both vehicles, $\eta_{\text{d}} = 1$ and $\eta_{\text{m}} = 0.96$ are set. The efficiencies of the DC-AC inverter were measured in (Geringer and Tober, 2012), resulting in $\eta_{\text{inv}} = 0.96$ (Nissan), and $\eta_{\text{inv}} = 0.91$ (Mitsubishi).

The efficiency of the high voltage battery is dependent on the outside temperature. The graphs in figure 3.4 show the actual values of the measurements. For the Nissan Leaf, η_{dis} is between $0.90 - 0.96$, and for the Mitsubishi i-MiEV, it is $0.88 - 0.95$.

In (Geringer and Tober, 2012), they were only able to measure the efficiency of the DC-DC converter of the Mitsubishi, with $\eta_{\text{acc}} = 0.83$. The value for Nissan is set to $\eta_{\text{acc}} = 1$ because measurements were not possible due to the specific construction. Heating and cooling use high voltage without converter, therefore their efficiency $\eta_{\text{hc}} = 1$.

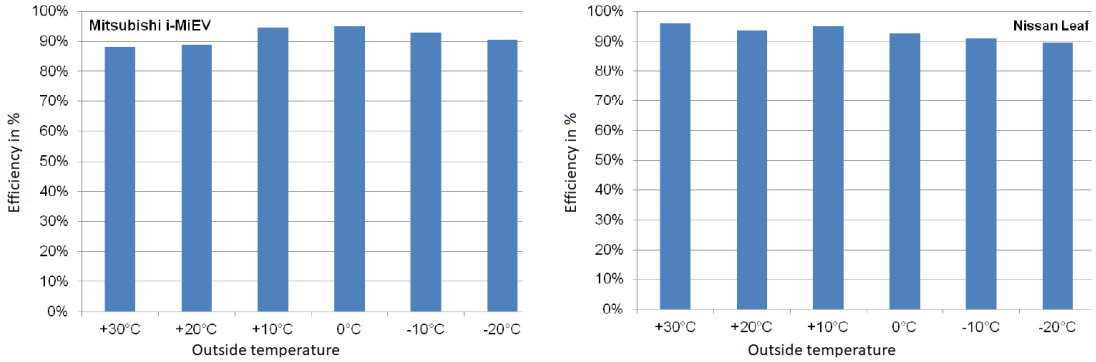

(a) Mitsubishi i-MiEV

(b) Nissan Leaf

Figure 3.4: The efficiencies of the batteries of the Nissan Leaf and Mitsubishi i-MiEV depending on the outside temperature, (Geringer and Tober, 2012) - edited

Table 3.5: Parameters of the two electric vehicles

		Nissan Leaf	Mitsubishi	
Dimensions				
Curb weight		1516	1090	kg
Mass with driver	m	1591	1165	kg
Drag coefficient	c_w	0.28	0.33	-
Width with mirrors		1967	1792	mm
Width w/o mirrors	w	1770	1475	mm
Height	h	1550	1610	mm
Cross sectional area	A	2.22	2.14	m^2
Accessory loads				
Heating	P_{heat}	90	95	W/°C
Cooling	P_{cool}	40	30	W/°C
Lights	P_{light}	48	38/127	W
Fan	P_{air}	62	48	W
Battery				
Capacity	SoC_{max}	24	16	kWh
Efficiencies				
Drive	η_{d}	1	1	
Motor	η_{m}	0.90	0.90	
Inverter DC-AC	η_{inv}	0.96	0.91	
Battery	η_{dis}	0.90-0.96	0.88-0.95	
Accessories DC-DC	η_{acc}	1	0.83	
Heating/Cooling	η_{hc}	1	1	

4 Results

4.1 Route Planning

The model and optimization algorithms introduced in chapter 3 have been tested with the help of MATLAB. Two different areas served as simple models of the street network. At first, the 'Wienerwald' area, which is in the west of Vienna, Austria, was chosen. Because of its pretty unique topography, the city of San Francisco, California, was the second example for testing the route planning algorithm.

4.1.1 Wienerwald, Austria

The street network covers the main roads of the Wienerwald area in the west of Vienna. The route planning does not include the city of Vienna, because it is an urban network with a lot of unknown properties such as traffic lights, zebra crossings, and traffic jams. The energy consumption and the journey time depend on all those factors too. The proposed model is quite simple and ignores those things, mainly because it is very hard to get the right data and information.

The area of the Wienerwald consists of some small towns and villages, but it is mostly woods and fields. It has a diverse topography with a lot of small hills. Therefore it seems like a good place to start with the testing. More mountainous areas would be interesting too, but they are not that suitable for this kind of route planning, because there is usually only one main road connecting two places, and other paths are no reasonable choices. This is the advantage of Wienerwald. It is a non-urban area with still quite a few route options to choose from. Figure 4.1 shows a screen-shot from Google Maps that includes this network.

The following places are part of the network: At first there is Auhof, which is still part of the city of Vienna, but in the very west. At Auhof the highway A1 starts, which connects Vienna and the city of Salzburg. The first section of A1 that terminates at Pressbaum is an edge of the network. It is possible to reach Pressbaum via Purkersdorf and Untertullnerbach as well.

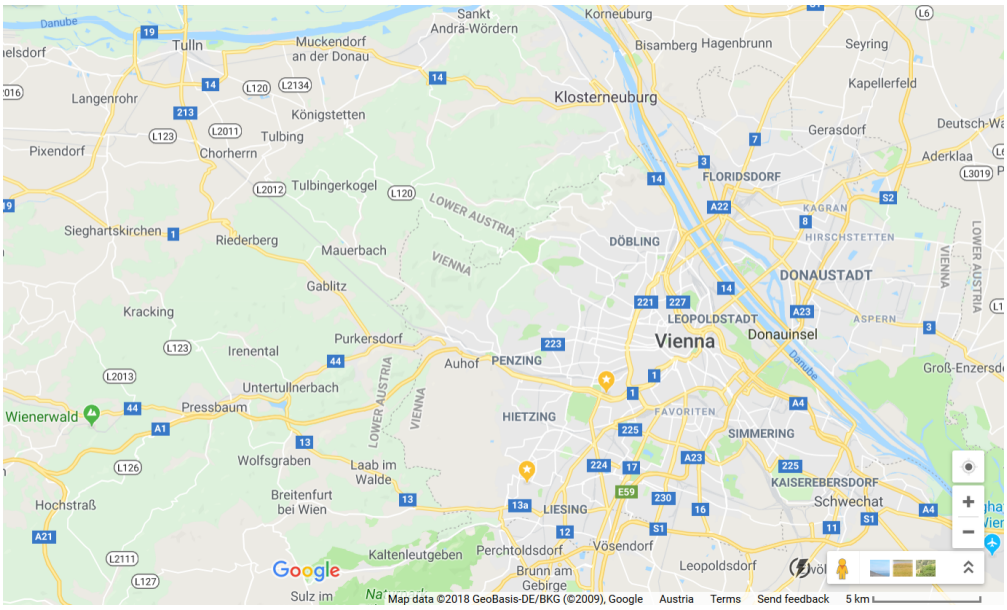

Figure 4.1: Vienna and Wienerwald (screen-shot from Google Maps)

Further north there is Sieghartskirchen and Reichersberg. Other towns are Mauerbach, Allhang, Maria Gugging, Tulbing, and Königstetten. This network has a total of 31 nodes and 41 edges.

The tests were done for different start and destination points. The multi-objective optimization as in section 3.4.5 was used to see which roads are picked when favoring one optimization variable. Since this is a real world street network, some trips have one optimal solution for all the scenarios. In many cases, the fastest route is the most energy efficient at the same time. For other cases, there is more than one option when planning the trip. Some interesting results were achieved with different weights on the optimization variables.

The optimization variables are:

- Energy consumption: The energy consumption of an electric vehicle is calculated according to the model in 3.2. The weight for this variable is γ.
- Journey time: The total time required to go from the start point to the destination. The length of the roads and the speed of the vehicle are derived from the network. The weight here is δ.
- Battery lifetime: In order to increase the battery's lifetime, the number of total charging and discharging cycles has to be reduced. The optimization variable is the absolute value of the energy that is either consumed or generated. The goal is to

minimize the energy flow. It is weighted with the factor $1-(\gamma+\delta)$, with $\gamma+\delta \leq 1$.

Different combinations of $\gamma = 0, 0.2, \ldots, 1$ and $\delta = 0, 0.2, \ldots, 1$ are tried out, while always obeying $\gamma + \delta \leq 1$. In the following sections it is analyzed how much the weights influence the choice of an optimal route by picking out two scenarios with different start and destination points.

Route: From Auhof to Sieghartskirchen

The first interesting result is the route from Auhof to Sieghartskirchen. Applying different weights to the optimization variables, the following two routes are obtained from the optimization problem:

(a) The first route goes via Purkersdorf, Allhang, and Reichersberg. It is the path from Auhof to Sieghartskirchen that has the shortest distance (see figure 4.2, blue).
(b) This route goes via highway A1 and Pressbaum. It is longer, but the vehicle is a lot faster on the highway than on the other roads that are passing small towns and villages. According to the results obtained in this work it is fastest route (see figure 4.2, red).

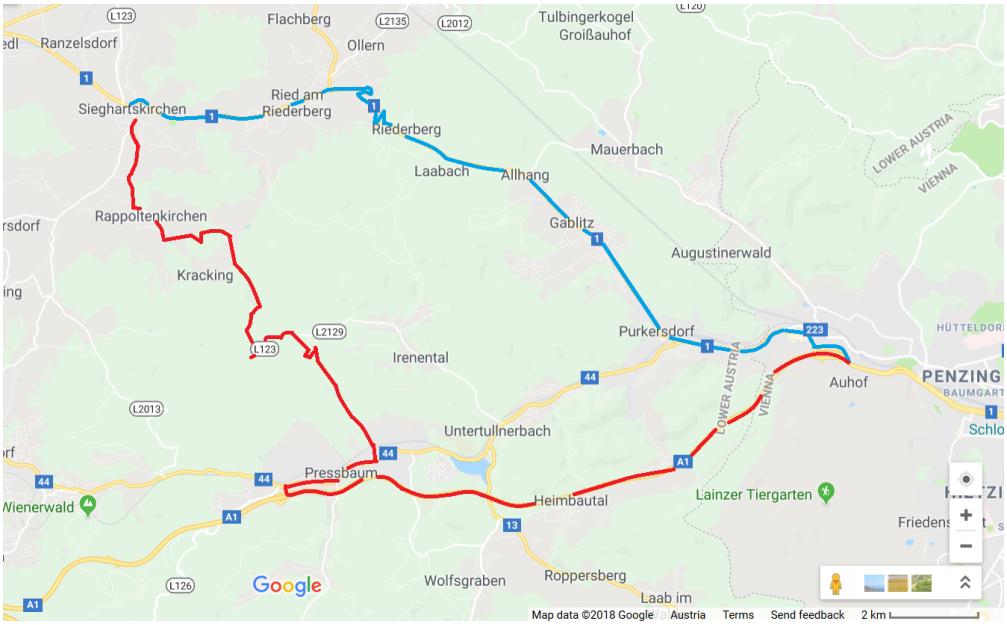

Figure 4.2: Results for Auhof to Sieghartskirchen (screen-shot from Google Maps - edited)

The multi-objective optimization, which puts emphasis on energy consumption, time, or cyclic lifetime, gives us the results in table 4.1 for the route planning. All the combinations of different values for γ and δ lead to the same result except for one.

The option of taking the highway and being slightly faster, by less than half a minute, is considered when $\delta = 1$. This means that when the multi-objective optimization turns into a single-objective optimization for the journey time, route (b) is chosen. All the other combinations have the same solution, which is route (a) via Purkersdorf, Allhang, and Reichersberg.

Table 4.1: Results for Auhof - Sieghartskirchen with Nissan Leaf at 20 °C

γ/δ	0	0.2	0.4	0.6	0.8	1
0	(a)	(a)	(a)	(a)	(a)	(b)
0.2	(a)	(a)	(a)	(a)	(a)	-
0.4	(a)	(a)	(a)	(a)	-	-
0.6	(a)	(a)	(a)	-	-	-
0.8	(a)	(a)	-	-	-	-
1	(a)	-	-	-	-	-

Figure 4.3 - 4.6 compare the two results in terms of topography, energy consumption, absolute energy consumption (for the cyclic lifetime of the battery), and time. It can be noticed that route (b) is a lot longer than route (a). Figure 4.3, where it shows the topography, it can be noticed that both routes have significant changes in altitude, yet the slope in Route (b) alternates a little bit more.

The energy consumption (see figure 4.4) and the absolute energy (figure 4.5) are a lot higher for route (b) as a result of the topography and - more important - as a result of the much longer distance.

The journey time (figure 4.6) is almost the same for both routes. It takes the vehicle 22.69 minutes on route (a) compared to 22.46 minutes on route (b). The difference in energy consumption on the other hand is more significant. Using the Nissan Leaf while having an outside temperature of 20 °C, where no heating or air condition is needed, the difference is around 2.88 kWh, according to the calculations.

This explains why the energy consumption is favored in all cases except for one ($\delta = 1$). If $\delta < 1$, the very significant difference in energy consumption influences the result automatically, even if γ is very small. The second best journey time is only about one percent slower, while the energy consumption of the is around 30% higher. Even with a δ of 0.99, the is result still in favor of the energy-optimal route.

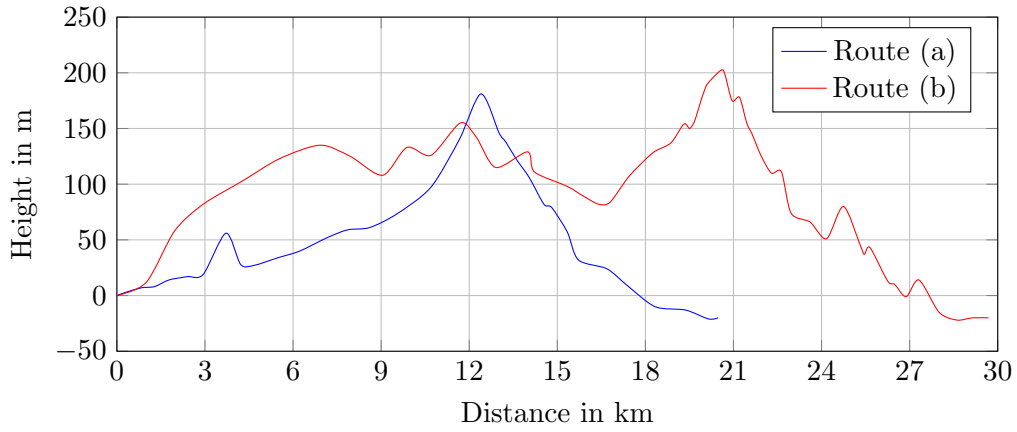

Figure 4.3: Topography of route (a) and route (b) from Auhof to Sieghartskirchen

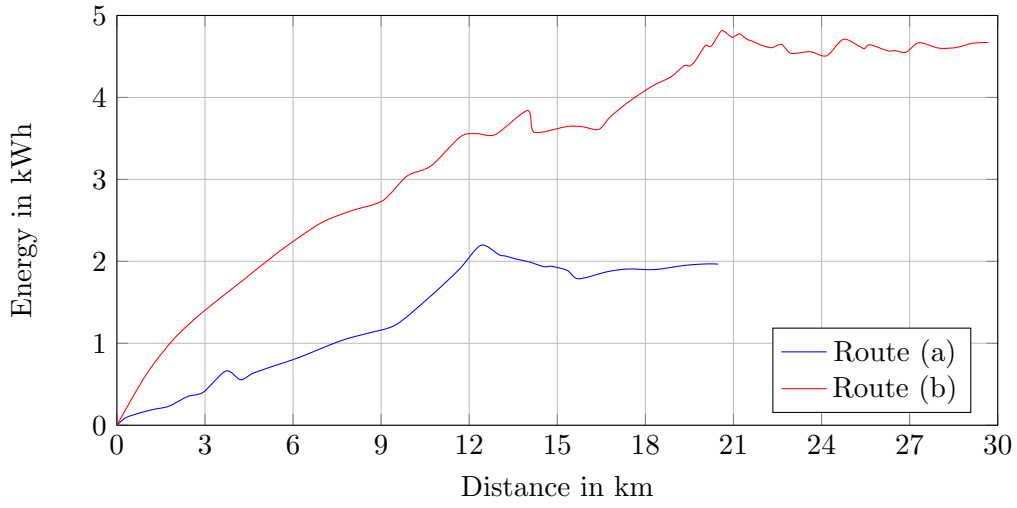

Figure 4.4: Energy consumption (cumulated) of route (a) and route (b) from Auhof to Sieghartskirchen

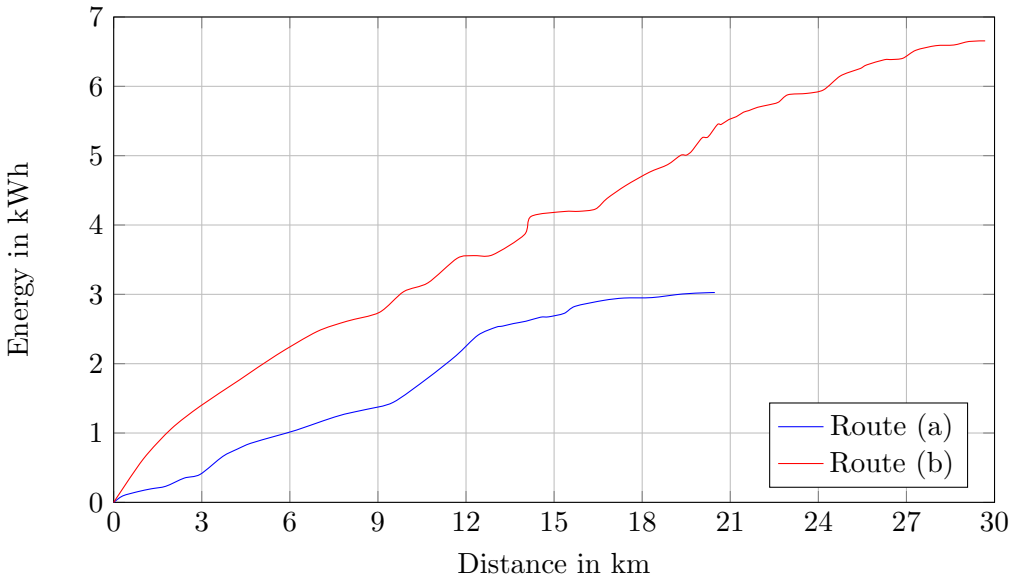

Figure 4.5: Absolute value (cumulated) of the energy consumed or regenerated of route (a) and route (b) from Auhof to Sieghartskirchen

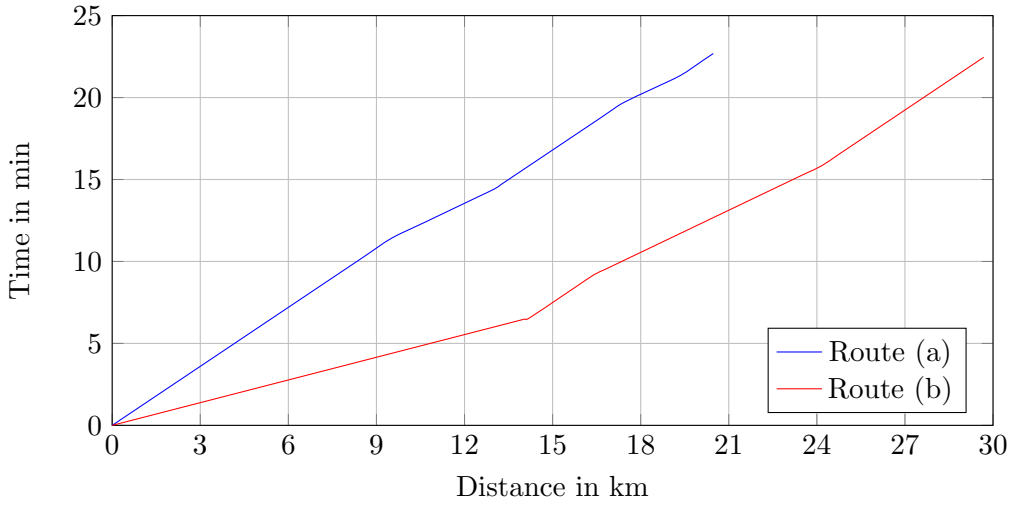

Figure 4.6: Journey time of route (a) and route (b) from Auhof to Sieghartskirchen

Route: From Passauerhof to Maria Gugging

The route planning from Passauerhof to Maria Gugging gives other interesting results. There are two different solutions of the multi-objective optimization with different weights on the optimization variables. At first, we will analyze the results obtained at an outside temperature of 20 °C with the Nissan Leaf. The routes are:

(a) The first path, where the electric vehicle needs the least amount of energy, starts at Passauerhof and goes via Katzlsdorf, Königstetten, and St. Andrä before it reaches the destination, Maria Gugging (see figure 4.7, blue).
(b) The other route passes some small villages (e.g. Unterkirchbach and Hintersdorf) until it reaches Maria Gugging (see figure 4.7, red). It is the fastest and shortest route at the same time and has much more variation in topography than (a).

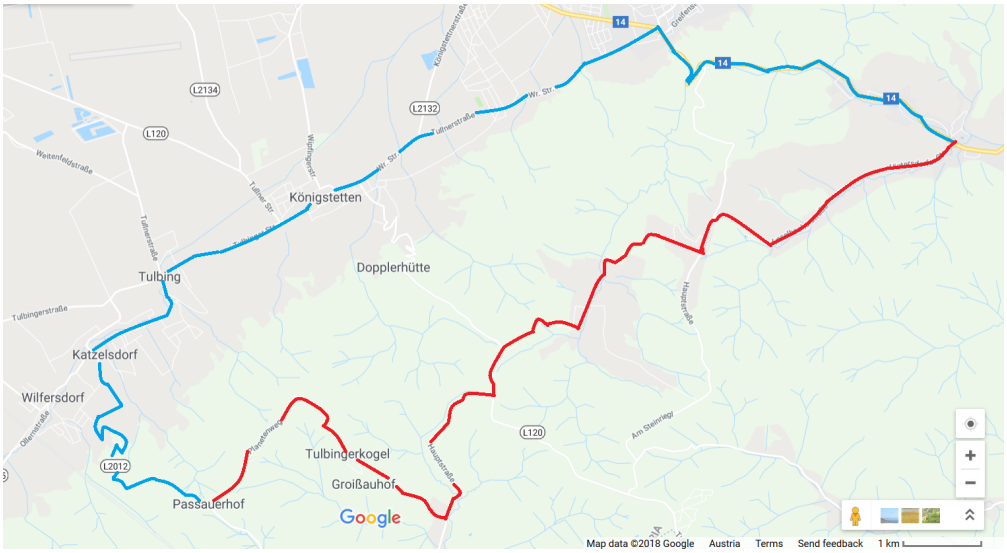

Figure 4.7: Results for Passauerhof to Maria Gugging (screen-shot from Google Maps - edited)

Table 4.2 presents the solutions from the multi-objective optimization for various combinations of the weights. It can be noticed that combinations with a low value for γ and δ result in option (a). This route has less variation in topography than (b), as it can be seen in figure 4.8. When γ and δ are small, the focus is on increasing the battery lifetime. In contrast to the optimization variable for energy consumption, where the regenerated energy has a negative sign and therefore helps minimizing the costs, the optimization variable that represents the battery lifetime takes the absolute value of the energy. The regenerated energy counts the same way as the consumed energy. Therefore driving downhill or braking increases the costs and is avoided by the optimization algorithm. A route that has little elevation up and down is preferred. It can be seen in figure 4.10

that the absolute value of the energy, which has either been consumed or regenerated, of route (a) is less than of route (b).

Table 4.2: Results for Passauerhof-Maria Gugging with Nissan Leaf at 20 °C

γ/δ	0	0.2	0.4	0.6	0.8	1
0	(a)	(a)	(a)	(b)	(b)	(b)
0.2	(a)	(a)	(a)	(b)	(b)	-
0.4	(a)	(a)	(b)	(b)	-	-
0.6	(a)	(a)	(b)	-	-	-
0.8	(a)	(b)	-	-	-	-
1	(a)	-	-	-	-	-

Combinations with a high value of δ lead to the fastest route, route (b). The difference in time is almost four minutes (see figure 4.11), which is about a quarter of the total journey time of route (b). The difference in energy consumption is a lot less significant (see figure 4.9). Choosing route (a), only a few Watt-hours are saved. Let's see what happens if the battery lifetime is neglected ($\gamma + \delta = 1$). A high value of γ and a small δ still lead to route (b), while only with $\gamma = 1$, route (a) is chosen. The explanation is similar to the case of Auhof to Sieghartskirchen, where the savings in journey time were insignificant compared to the savings in energy consumption. In this case now, the journey time outweighs the energy consumption.

It is also interesting to see when the vehicle is charging or when it is discharging. Figure 4.12 shows the charging and discharging events of route (a), and figure 4.13 of route (b). This is done by showing when the energy E is positive (discharging) or negative (charging), see (3.22). The graphs only show the (dis)charging events due to elevation, not due to braking or acceleration. The electric vehicle changes between charging and discharging mode slightly more often on Route (b) than on Route (a). This charging/discharging frequency could also be included in the task of increasing the battery lifetime, although this work only focuses on the amount of energy flow.

In the next step, the tests are done for a different outside temperature. During winter, the temperatures can fall below zero in Austria, which means that the passengers in the vehicle want heating. The Nissan Leaf's power demand of the heating is $P_{\text{heat}} = 90\,\text{W}/^\circ\text{C}$ according to the measurements in (Geringer and Tober, 2012). The tests with 20 °C did not include heating or cooling, because they are not necessary. The energy consumption is expected to rise with cooler temperatures. How this can influence the results of the multi-objective optimization we are able to see now.

Setting the outside temperature to $T = -10^\circ\text{C}$, we have

$$P_{\text{hc}} = P_{\text{heat}}(T_0 - T) = 1800\,\text{W}, \tag{4.1}$$

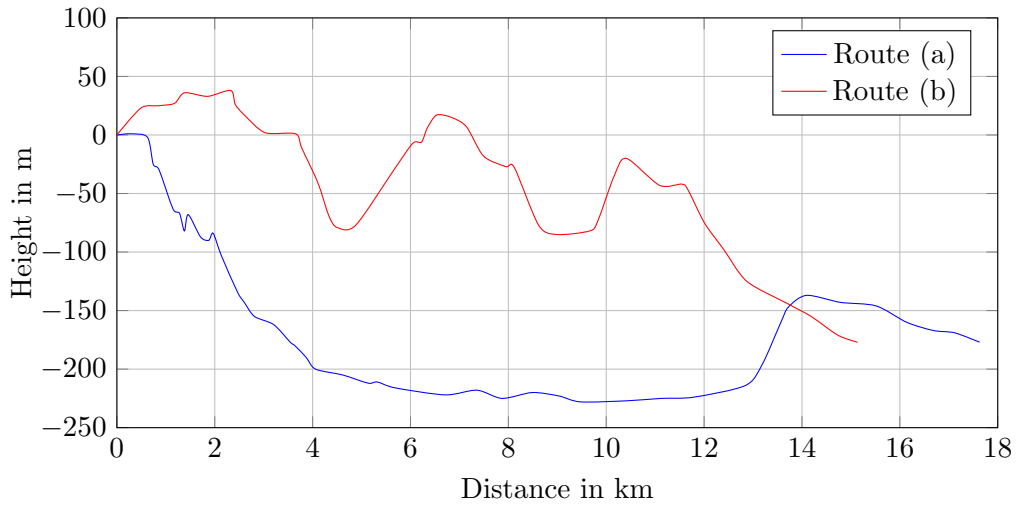

Figure 4.8: Topography of route (a) and route (b) from Passauerhof to Maria Gugging

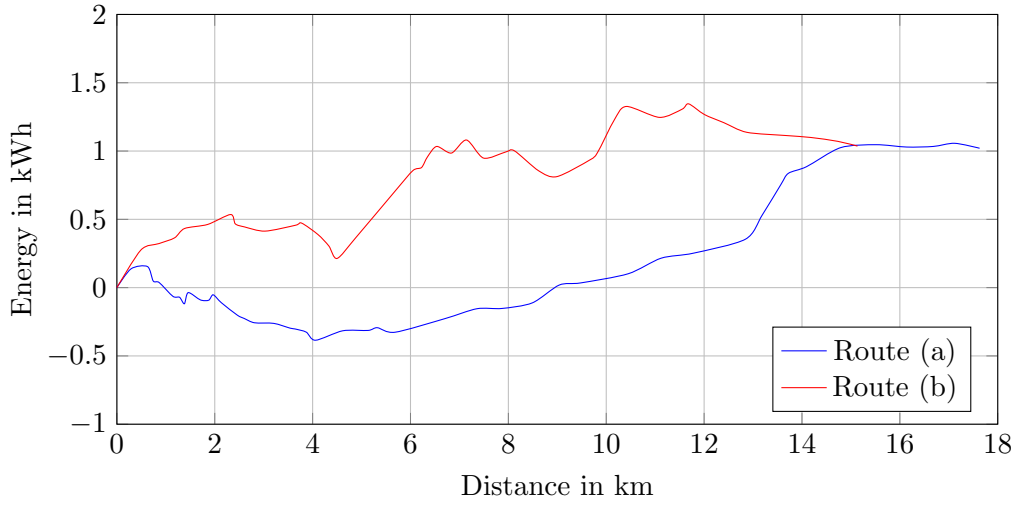

Figure 4.9: Energy consumption (cumulated) of route (a) and route (b) from Passauerhof to Maria Gugging

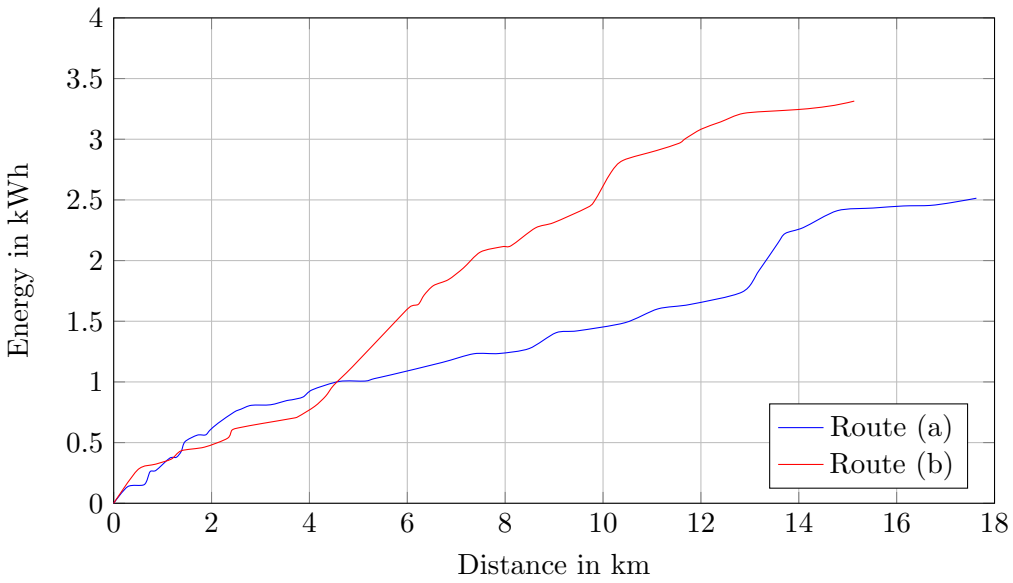

Figure 4.10: Absolute value (cumulated) of the energy consumed or regenerated of route (a) and route (b) from Passauerhof to Maria Gugging

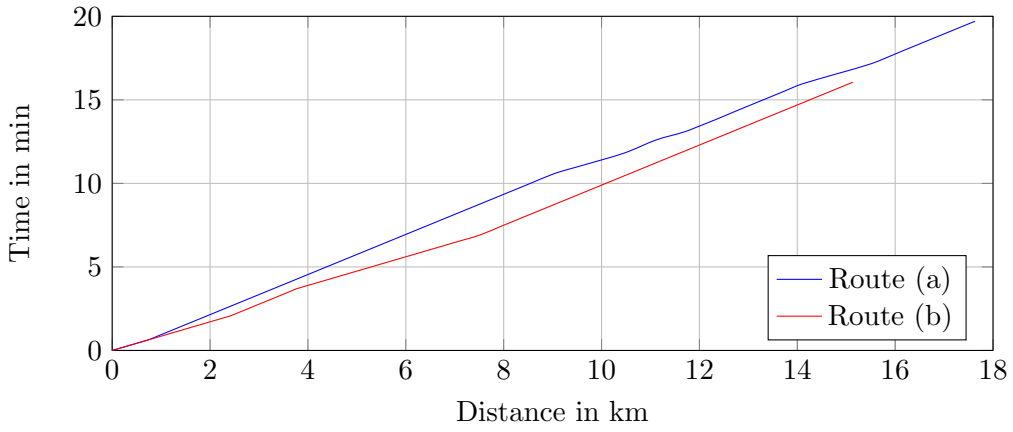

Figure 4.11: Journey time of route (a) and route (b) from Passauerhof to Maria Gugging

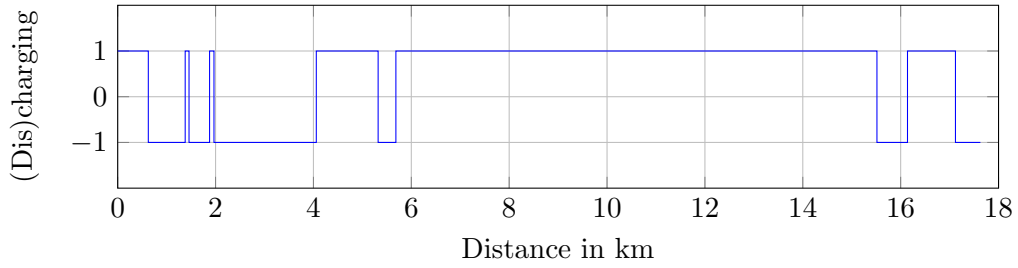

Figure 4.12: Charging and discharging events of route (a) from Passauerhof to Maria Gugging

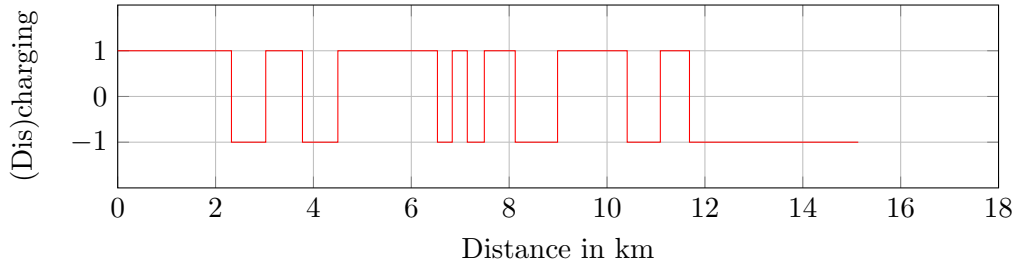

Figure 4.13: Charging and discharging events of route (b) from Passauerhof to Maria Gugging

with $T_0 = 20°C$. The journey time is almost 20 minutes, such that about 0.6 kWh are used only for heating, while this is a relatively short trip. Also, battery efficiencies are decreasing at such low temperatures (see figure 3.4). Table 4.2 shows the results of various combinations of the optimization weights.

Table 4.3: Results for Passauerhof - Maria Gugging with Nissan Leaf at −10 °C

γ/δ	0	0.2	0.4	0.6	0.8	1
0	(a)	(a)	(b)	(b)	(b)	(b)
0.2	(a)	(a)	(b)	(b)	(b)	-
0.4	(a)	(b)	(b)	(b)	-	-
0.6	(b)	(b)	(b)	-	-	-
0.8	(b)	(b)	-	-	-	-
1	(b)	-	-	-	-	-

Those results are not surprising when we know that the energy consumption of all accessories including heating and cooling are time-dependent. This factor makes fast routes more attractive also when looking at energy-optimal route planning. In this case, route (a), which had less energy consumption at 20 °C, now needs more energy than route (b), making route (b) the most energy and time efficient route (see figure 4.14).

Only when the focus is on the cyclic lifetime of the battery (low γ and δ), route (a) is chosen because of the topography, as explained previously. It can be seen in figure 4.15 that the cumulated absolute energy consumption and regeneration of route (a) is still less than of route (b), but the difference is smaller at $-10\,°C$ compared to $20\,°C$.

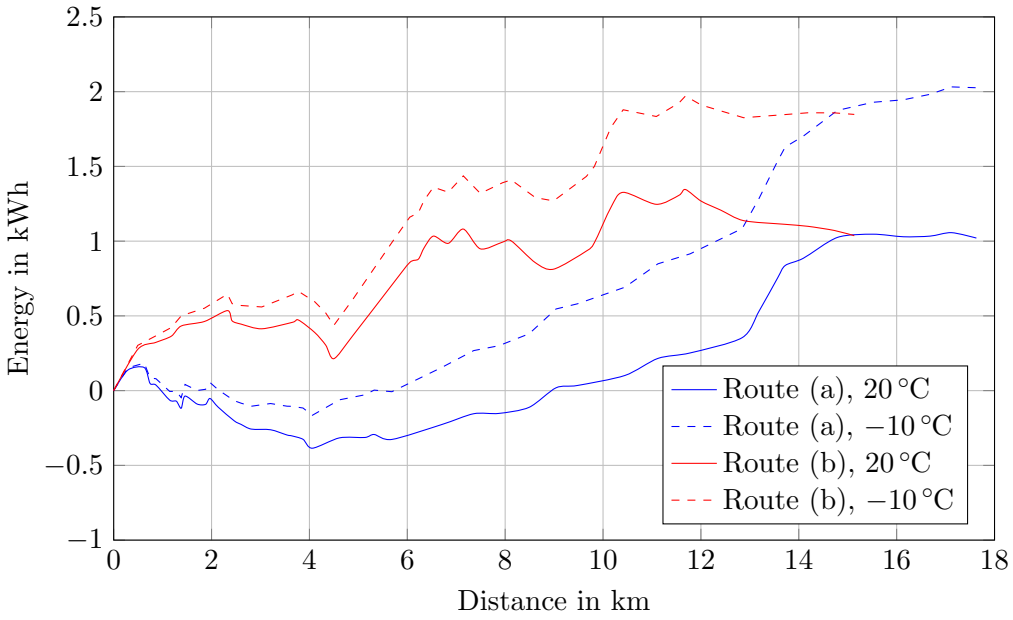

Figure 4.14: Energy consumption (cumulated) of route (a) and route (b) from Passauerhof to Maria Gugging comparing the outside temperatures of $20\,°C$ and $-10\,°C$

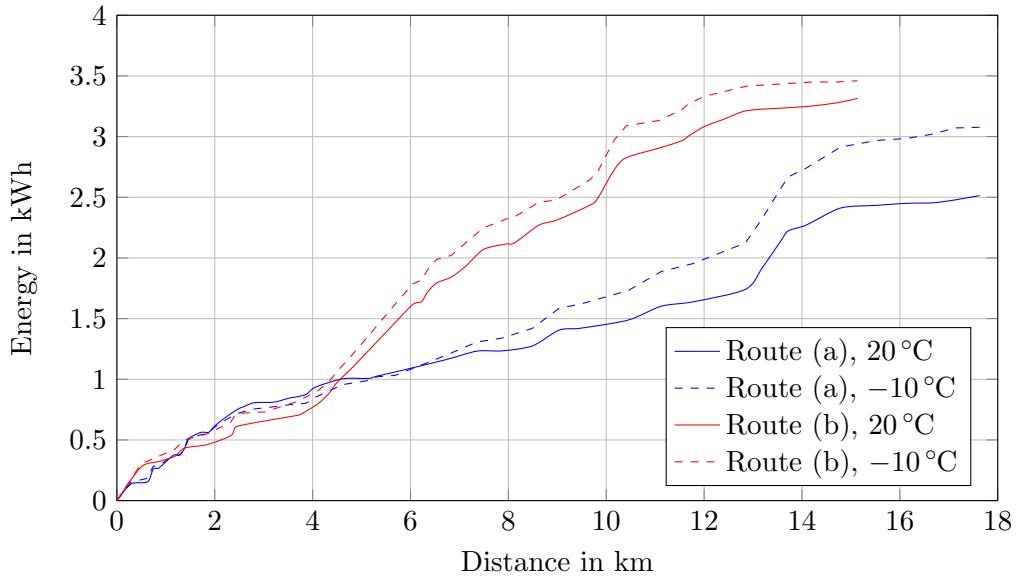

Figure 4.15: Absolute value (cumulated) of the energy consumed or regenerated of route (a) and route (b) from Passauerhof to Maria Gugging comparing the outside temperatures of 20 °C and −10 °C

4.1.2 San Francisco, California

Next, the tests were done for the city of San Francisco, California, because of its interesting topography. The street network of San Francisco is fundamentally different from the street network of Wienerwald. It is an urban area with a high density of roads (see figure 4.16). The network is shaped like a grid with perpendicular streets. Each intersection represents a node of the network.

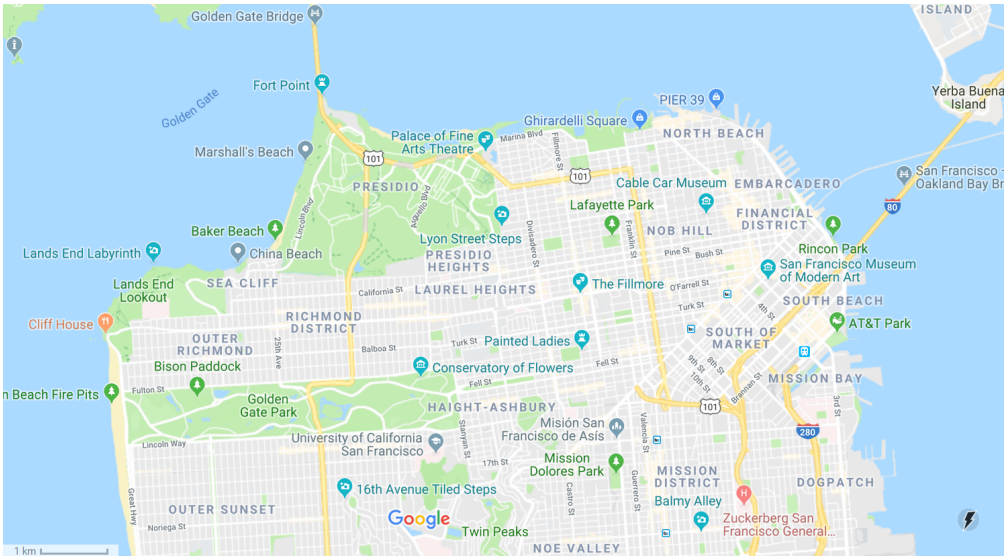

Figure 4.16: The city of San Francisco, California (Screen-shot from Google Maps)

Because of the high density of roads, there is also a high number of nodes. Therefore only a small part of downtown San Francisco was selected in order to keep the network more compact.

Modeling an urban street network can be challenging because it has a lot of factors that are hard to predict. Traffic would be the first thing that comes into mind. When searching for the fastest route, the current traffic situation is a main factor. Traffic lights will also influence the results. The fastest route from the calculations can turn out to be not that fast if the timing of the traffic lights was bad. Other factors would be zebra crossings, stop signs, bus stops, et cetera.

Not only the journey time, but also the energy consumption is influenced by those factors. Nevertheless, influences of traffic are neglected for simplification in this work. The deviation from the real duration of the journey is accepted and the focus will be on the energy consumption and battery lifetime, where the topography of the city has the most effect on.

Route: From Pier 39 to Russian Hill

Let's start with some interesting results. The journey starts close to Pier 39, at the corner Beach Street/Grant Avenue. The destination point is Union Street/Hyde Street, close to Russian Hill. For all combinations of the multi-objective optimization weights, the same result is obtained (see figure 4.17). Going in the opposite direction, from Russian Hill to Pier 39, there are two results. For all combinations of γ and δ, except for $\delta = 1$, we have the result in figure 4.18. Only for $\delta = 1$, we have the same result as before from 4.17. This result is for time-optimization only, therefore not significant, since the calculation of the journey time without knowing the traffic situation is rather vague.

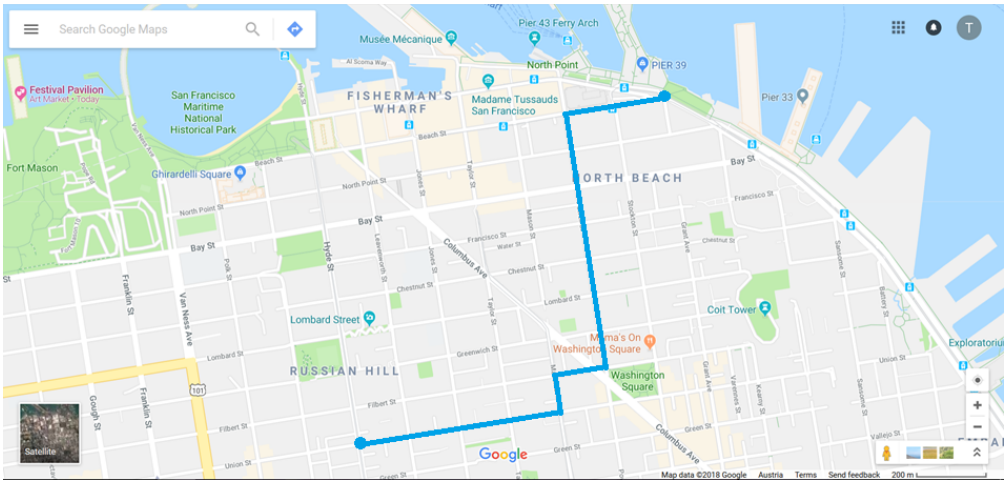

Figure 4.17: Result for Pier 39 to Russian Hill (screen-shot from Google Maps - edited)

Figure 4.19 shows the topography of the two scenarios: Going from Pier 39 to Russian Hill (Union/Hyde Street) and the return. The energy consumption on both trips (see figure 4.20) is strongly dependent on the topography. Since Pier 39 is almost at sea level, going to Russian Hill takes a lot of energy, while the electric vehicle regenerates energy by going down to Pier 39.

It is interesting to see in figure 4.21 that the absolute energy of the return trip is a lot less. At low speed, the rolling resistance is dominant, while the air resistance is less significant. The energy that is regenerated when driving downhill is less than the energy that is needed to go uphill because of the rolling resistance and losses due to the efficiencies of the electric vehicle.

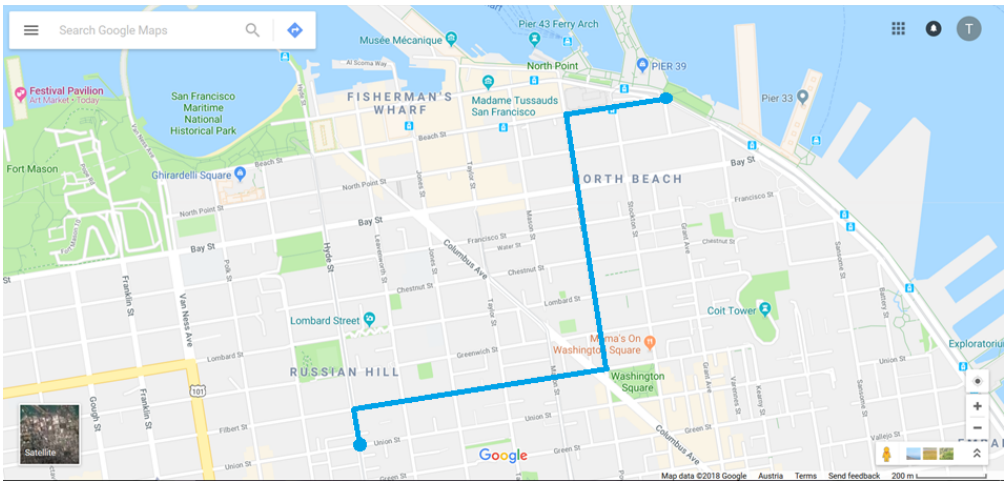

Figure 4.18: Result for Russian Hill to Pier 39 (screen-shot from Google Maps - edited)

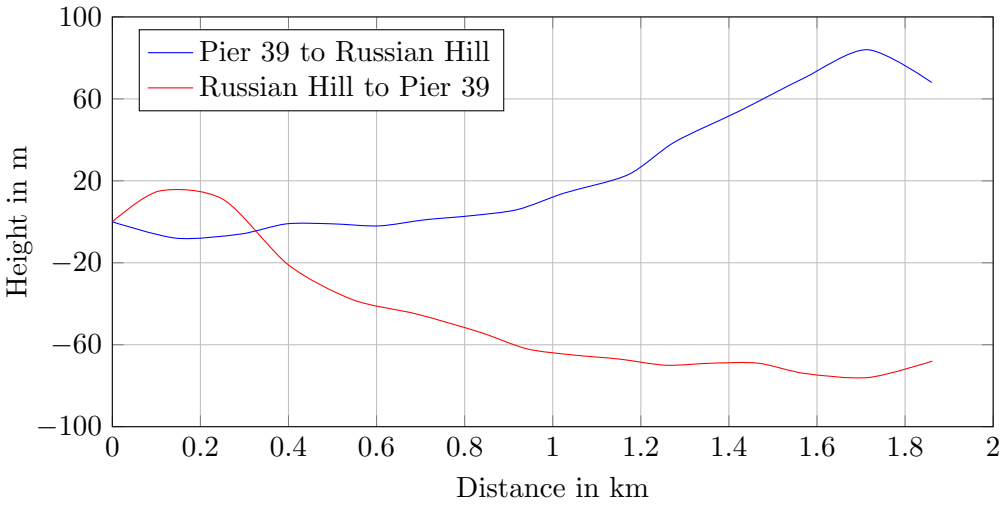

Figure 4.19: Topography of Pier 39 to Russian Hill and back

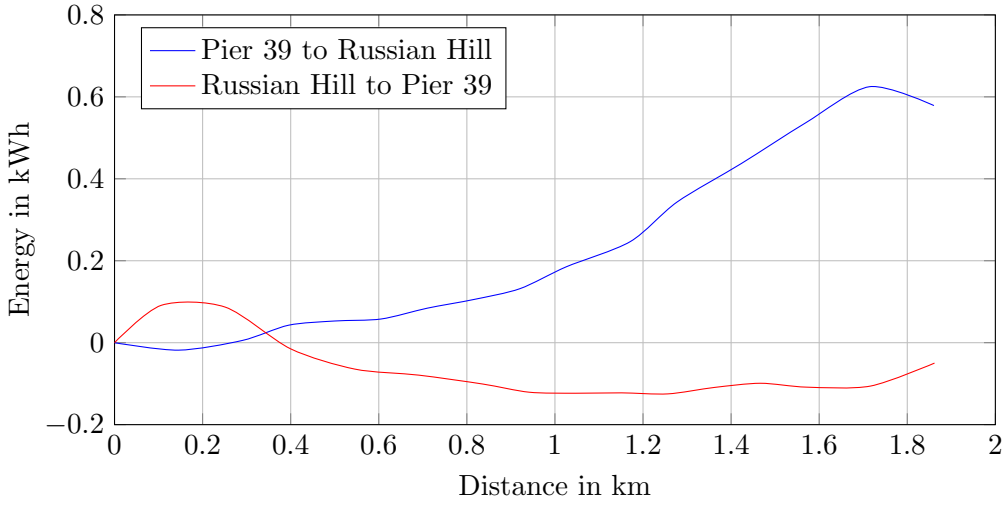

Figure 4.20: Energy consumption (cumulated) of Pier 39 to Russian Hill and back

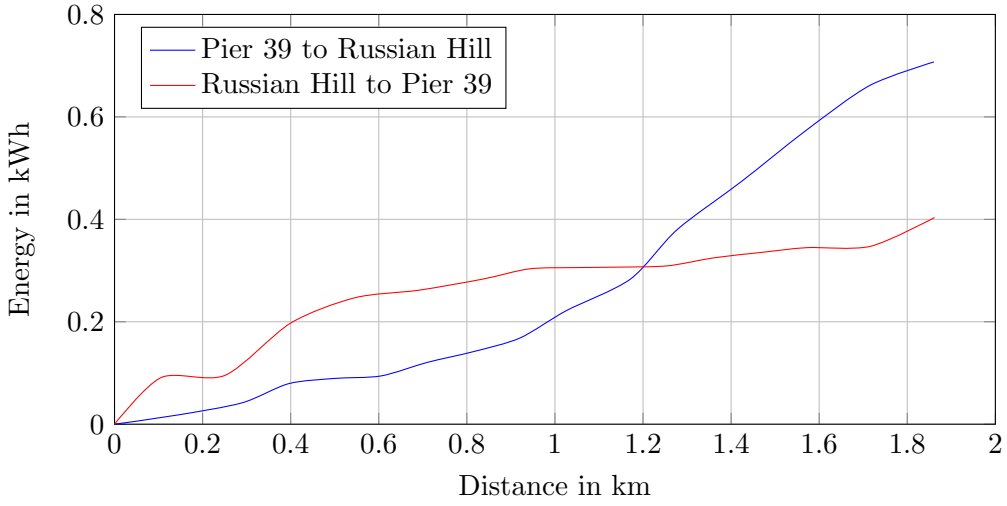

Figure 4.21: Absolute value (cumulated) of the energy consumed or regenerated of Pier 39 to Russian Hill and back

Route: From Union/Hyde Street to Lombard/Mason Street

Now we consider a relatively short trip from Union Street/Hyde Street to Lombard Street/Mason Street. The multi-objective optimization results in four different solutions:

(a) Goes via Filbert and Powell Street (see figure 4.22).
(b) Goes via Filbert, Greenwich, James, and Lombard Street (see figure 4.23).
(c) Goes via Filbert, Taylor, and Lombard Street (see figure 4.24).
(d) Goes via Leavenworth, Greenwich, James, and Lombard Street (see figure 4.25).

Table 4.4 shows that the optimization problem mostly results in route (b). With $\gamma = 0$ and $\delta = 0$, route (a) is chosen, while with $\gamma = 0.2$ and $\delta = 0$, route (c) is the solution. Route (d) is the result of $\delta = 1$, therefore it is the time-optimal path. As mentioned before, the calculation of the journey time is not very accurate. The focus will lie on optimization results for $\delta = 0$.

Table 4.4: Results for Union/Hyde Street-Lombard/Mason Street with Nissan Leaf

γ/δ	0	0.2	0.4	0.6	0.8	1
0	(a)	(b)	(b)	(b)	(b)	(d)
0.2	(c)	(b)	(b)	(b)	(b)	-
0.4	(b)	(b)	(b)	(b)	-	-
0.6	(b)	(b)	(b)	-	-	-
0.8	(b)	(b)	-	-	-	-
1	(b)	-	-	-	-	-

The results that are discussed are route (a), route (b), and route (c). The first thing that can be noticed when looking at the topography in figure 4.26 and the energy consumption in figure 4.27 is that the energy consumption depends a lot on the elevation, since the shape of the curves is similar. Route (c) is the most energy efficient one and route (a) has the smallest absolute energy consumption and regeneration (see figure 4.28).

These results show that the difference between the paths is not too significant, but it gives an impression on how the route planning would work for longer trips in the city.

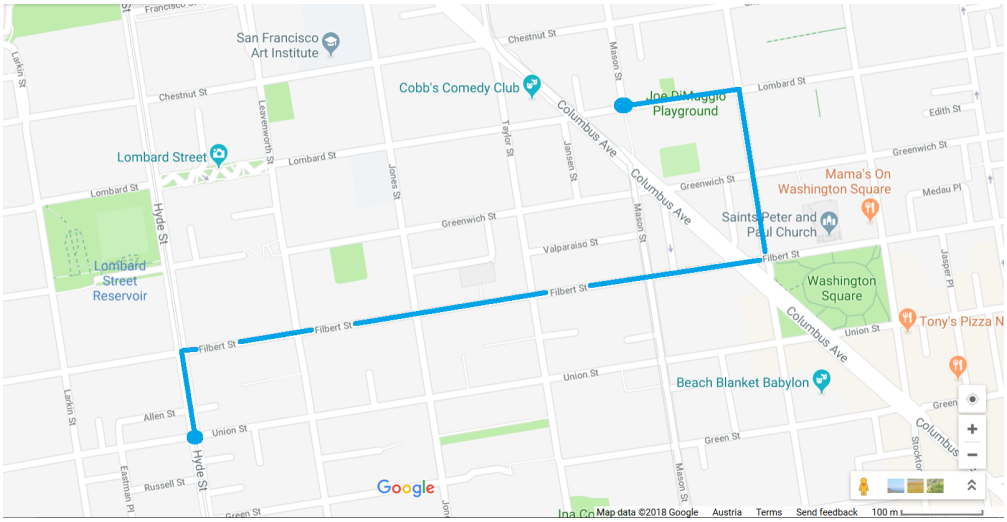

Figure 4.22: Route (a) for Union/Hyde Street to Lombard/Mason Street (screen-shot from Google Maps - edited)

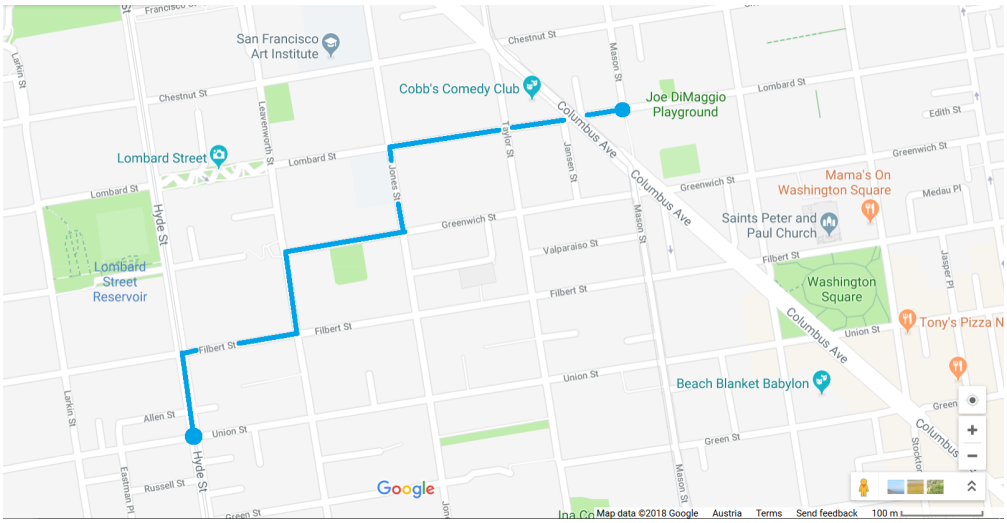

Figure 4.23: Route (b) for Union/Hyde Street to Lombard/Mason Street (screen-shot from Google Maps - edited)

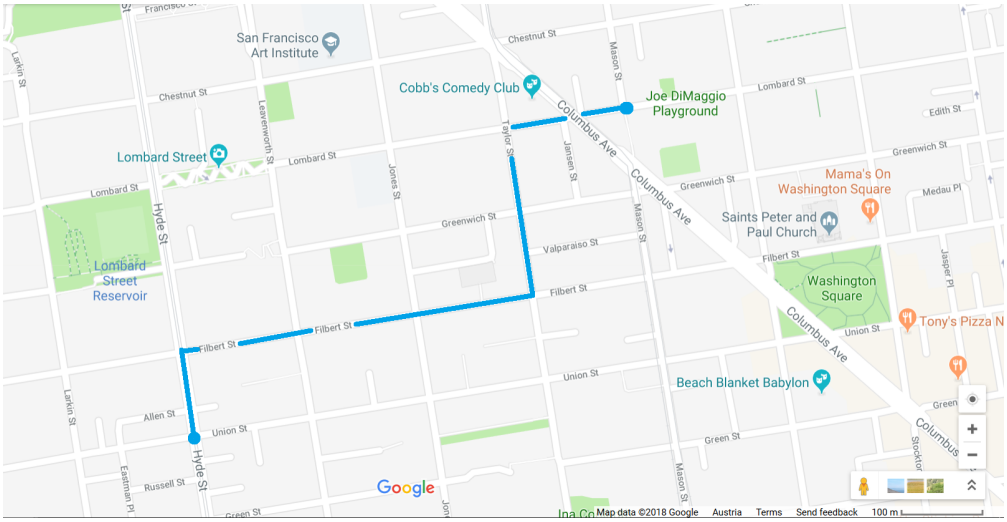

Figure 4.24: Route (c) for Union/Hyde Street to Lombard/Mason Street (screen-shot from Google Maps - edited)

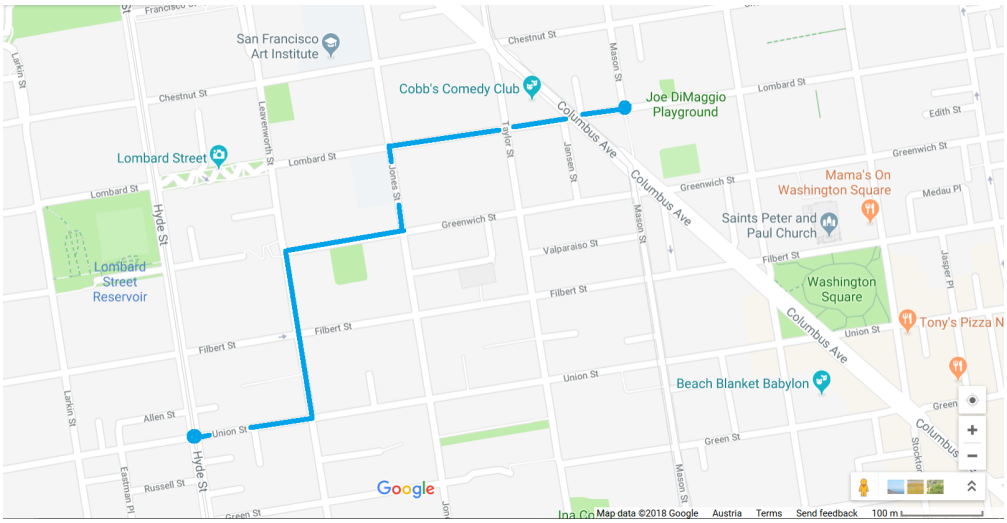

Figure 4.25: Route (d) for Union/Hyde Street to Lombard/Mason Street (screen-shot from Google Maps - edited)

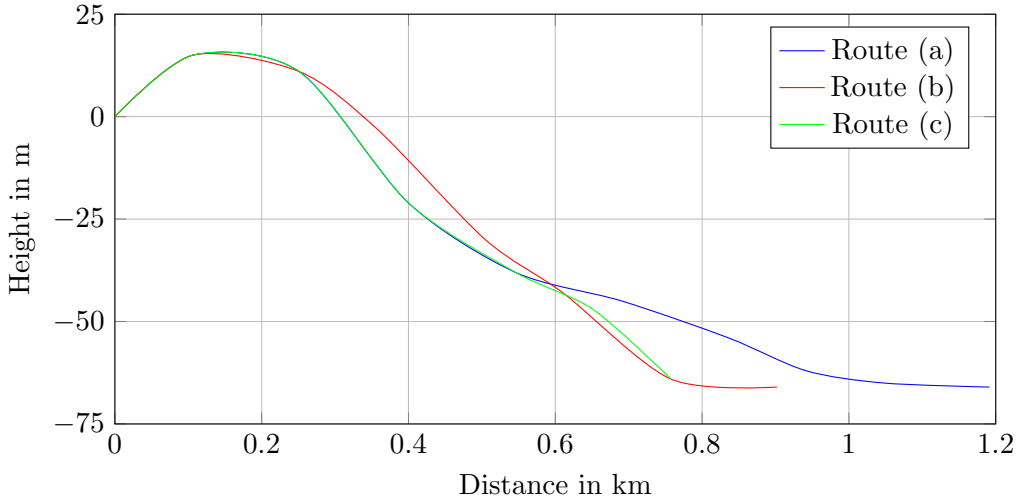

Figure 4.26: Topography of Union/Hyde Street to Lombard/Mason Street

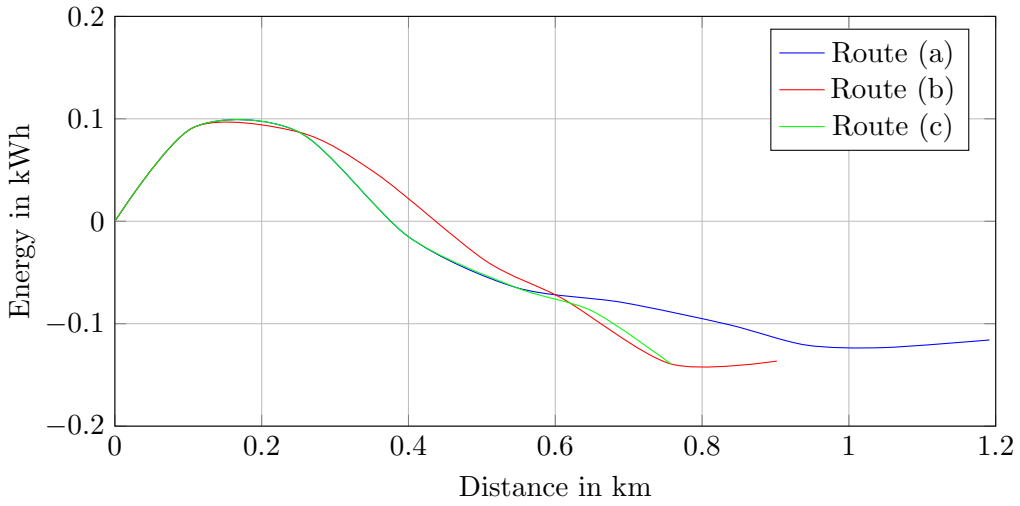

Figure 4.27: Energy consumption (cumulated) of Union/Hyde Street to Lombard/Mason Street

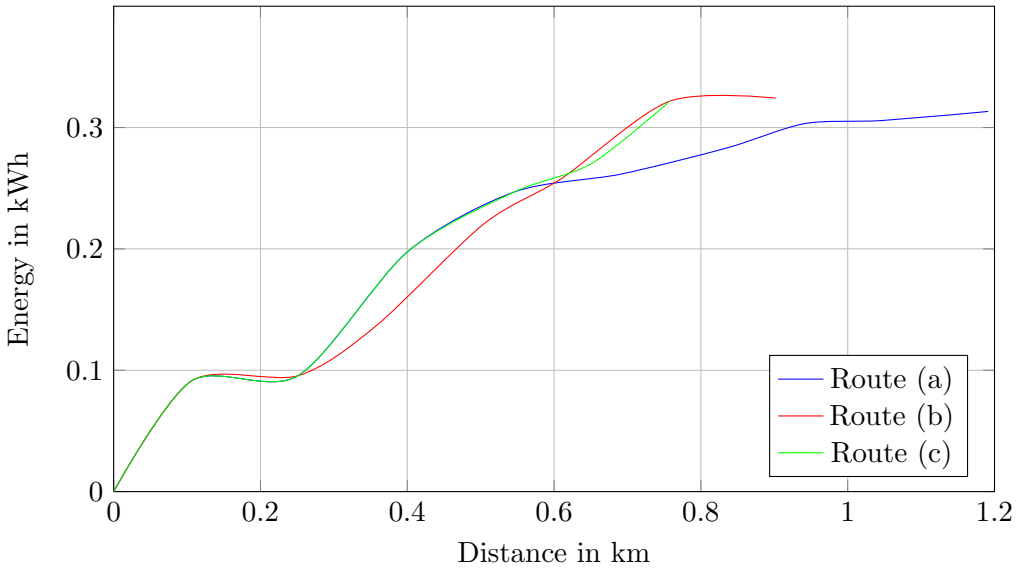

Figure 4.28: Absolute value (cumulated) of Union/Hyde Street to Lombard/Mason Street

5 Sensitivity Analysis

5.1 Comparing Nissan Leaf and Mitsubishi i-MiEV

In this section the results of two different electric vehicles are compared. In chapter 4 the tests were done with only one vehicle, the Nissan Leaf. In this part the Mitsubishi i-MiEV is added, with its characteristics as described in section 3.5. The Mitsubishi has almost 30% less weight, but the c_w-value is higher and the efficiencies are lower.

Wienerwald

Testing the same scenario as in section 4.1.1, from Passauerhof to Maria Gugging with the Mitsubishi i-MiEV, the same two routes are obtained from the optimization:

(a) Starts at Passauerhof and goes via Katzlsdorf, Königstetten, and St. Andrä before it reaches the destination, Maria Gugging (blue in figure 4.7).
(b) Starts at Passauerhof, then continues via Unterkirchbach and Hintersdorf on its way to Maria Gugging (red in figure 4.7).

Let's start with an outside temperature of 20 °C. In table 5.1 the results for Nissan Leaf and Mitsubishi i-MiEV are compared. The results of the Nissan have already been discussed in section 4.1.1. In figure 5.1 it can be seen that the energy consumption on both route (a) and route (b) is higher when driving the Mitsubishi despite having less weight. Another interesting finding is that the cumulated absolute value of the consumed and regenerated energy of the Mitsubishi is smaller compared to Nissan on both paths, while the normal energy consumption is the opposite. The regenerated energy must be the reason for those differences.

The only result that changed compared to Nissan is for $\gamma = 0.2$ and $\delta = 0.4$. The absolute energy has the weight of $1 - (\gamma + \delta) = 0.4$ in this scenario. The explanation could be found in figure 5.2, because the difference between route (a) and route (b) is smaller for the Mitsubishi than it was for the Nissan. Apparently it is small enough now that the time difference between the paths is more significant.

Table 5.1: Results for Passauerhof-Maria Gugging at 20 °C

(a) Nissan Leaf

γ/δ	0	0.2	0.4	0.6	0.8	1
0	(a)	(a)	(a)	(b)	(b)	(b)
0.2	(a)	(a)	**(a)**	(b)	(b)	-
0.4	(a)	(a)	(b)	(b)	-	-
0.6	(a)	(a)	(b)	-	-	-
0.8	(a)	(b)	-	-	-	-
1	(a)	-	-	-	-	-

(b) Mitsubishi i-MiEV

γ/δ	0	0.2	0.4	0.6	0.8	1
0	(a)	(a)	(a)	(b)	(b)	(b)
0.2	(a)	(a)	**(b)**	(b)	(b)	-
0.4	(a)	(a)	(b)	(b)	-	-
0.6	(a)	(a)	(b)	-	-	-
0.8	(a)	(b)	-	-	-	-
1	(a)	-	-	-	-	-

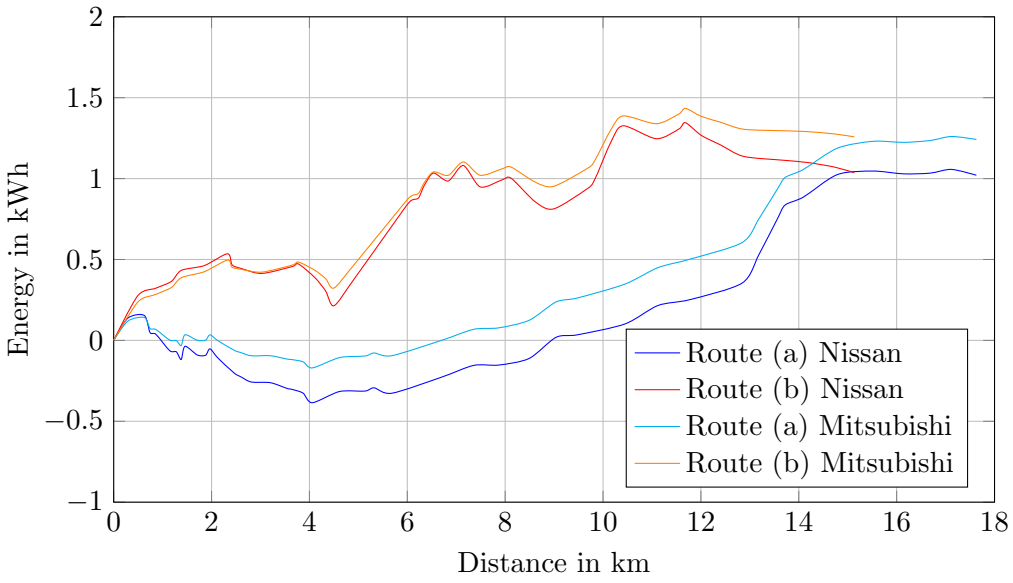

Figure 5.1: Energy consumption (cumulated) of route (a) and route (b) from Passauerhof to Maria Gugging comparing Nissan Leaf and Mitsubishi i-MiEV at 20 °C

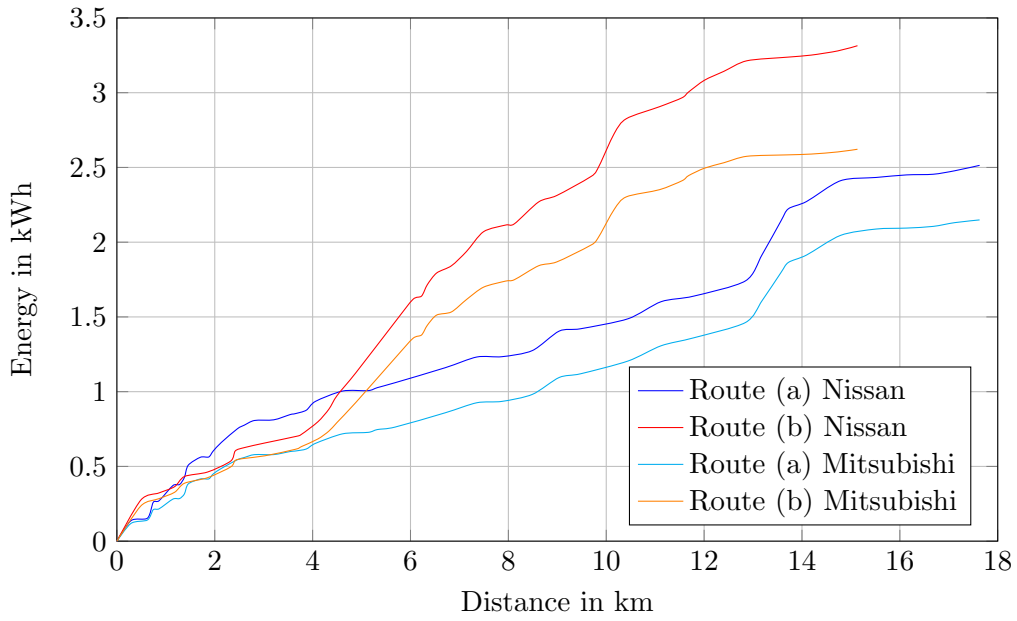

Figure 5.2: Absolute value (cumulated) of the energy consumed or regenerated of route (a) and route (b) from Passauerhof to Maria Gugging comparing Nissan Leaf and Mitsubishi i-MiEV at 20 °C

The next step compares the vehicles with a different outside temperature. As in section 4.1.1, the tests were done for −10 °C. Table 5.3 shows the results of both vehicles with different weights for the multi-objective optimization. In figure 5.3 it can be seen that the energy consumption of route (a) is higher than of route (b) for both vehicles. For the absolute energy in figure 5.4 it can be noticed that in case of the Mitsubishi, the values for route (a) and route (b) are almost equal now, leading to route (b) as the result of most combinations. Route (a) is still a little lower, therefore with $\gamma = 0$ and $\delta = 0$, route (a) is chosen.

Table 5.3: Results for Passauerhof-Maria Gugging at −10 °C

(a) Nissan Leaf

γ/δ	0	0.2	0.4	0.6	0.8	1
0	(a)	**(a)**	(b)	(b)	(b)	(b)
0.2	**(a)**	**(a)**	(b)	(b)	(b)	-
0.4	**(a)**	(b)	(b)	(b)	-	-
0.6	(b)	(b)	(b)	-	-	-
0.8	(b)	(b)	-	-	-	-
1	(b)	-	-	-	-	-

(b) Mitsubishi i-MiEV

γ/δ	0	0.2	0.4	0.6	0.8	1
0	(a)	**(b)**	(b)	(b)	(b)	(b)
0.2	**(b)**	**(b)**	(b)	(b)	(b)	-
0.4	**(b)**	(b)	(b)	(b)	-	-
0.6	(b)	(b)	(b)	-	-	-
0.8	(b)	(b)	-	-	-	-
1	(b)	-	-	-	-	-

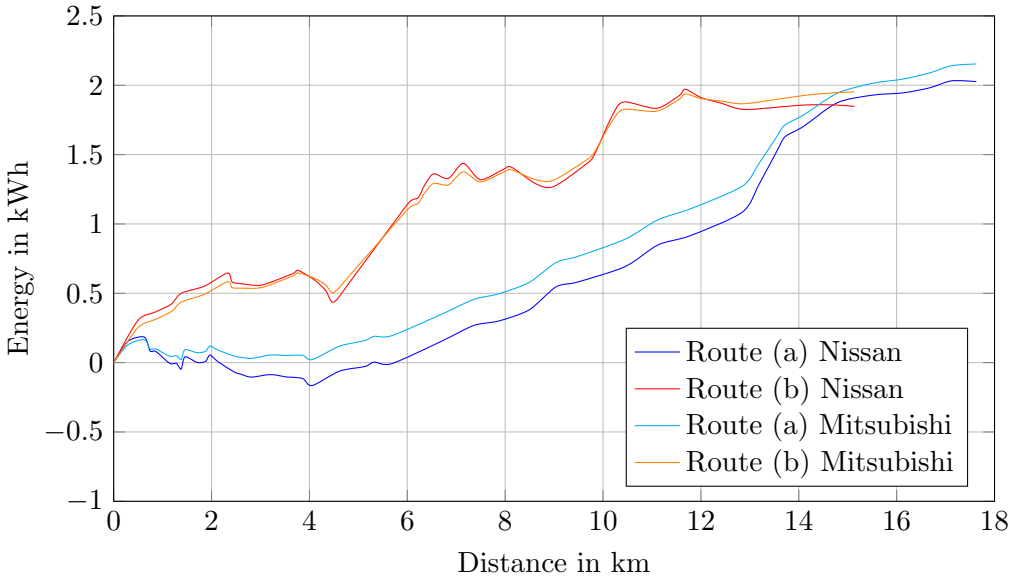

Figure 5.3: Energy consumption (cumulated) of route (a) and route (b) from Passauerhof to Maria Gugging comparing Nissan Leaf and Mitsubishi i-MiEV at −10 °C

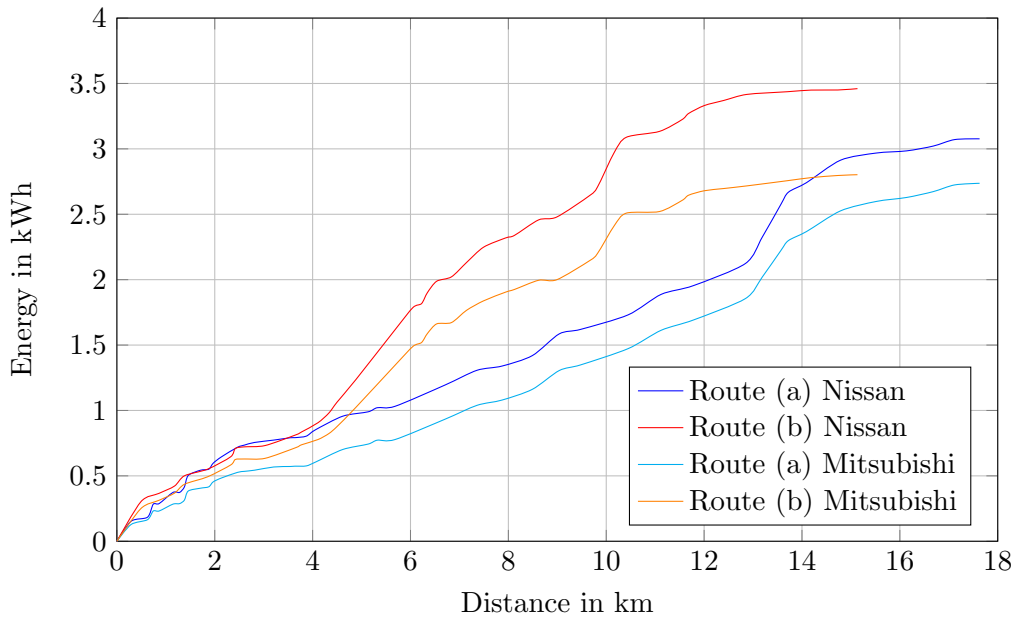

Figure 5.4: Absolute value (cumulated) of the energy consumed or regenerated of route (a) and route (b) from Passauerhof to Maria Gugging comparing Nissan Leaf and Mitsubishi i-MiEV at −10 °C

5.2 Different Weather Conditions

All previous tests have been done with minimal accessory loads, only using headlights, the fan, and heating if necessary due to a low outside temperature. When certain conditions are met, this is not accurate anymore. For example when there is rain, the windshield wipers are used. When there is fog, the fog lights are necessary. If humidity is high, the fans should operate on settings with high power.

Now the following scenario is tested. It is assumed to be night time, so headlights, license plate lights, and lights for the instrument panel are necessary. The outside temperature is 10 °C and according to (3.75), the power for the heating is

$$P_{\mathrm{hc}} = P_{\mathrm{heat}}(T_0 - T) = 900\,\mathrm{W}, \tag{5.1}$$

with $P_{\mathrm{heat}} = 90\,\mathrm{W}$. It is assumed to be foggy as well, making fog lights and rear fog lights necessary. Table 5.5 shows all the accessories that are used in this scenario and their power consumption.

The results in table 5.7b are obtained and compared to the results with an outside temperature of 20 °C in table 5.7a, with route (a) and route (b) as explained in section 5.1. The difference in energy consumption is about 0.1 kWh, such that route (b) is the

Table 5.5: Accessory loads for different weather conditions

Load	Value
Heating	900 W
Dimmed headlights	48 W
Instrument panel lights	22 W
License plate lights	30 W
Rear window heating	178 W
Fog lights	110 W
Rear fog lights	21 W
Fan	143 W

fastest and most energy efficient route. Only when the optimization algorithm focuses on the cyclic lifetime of the battery, route (a) is chosen because of the topography (compare figure 4.8). Figure 5.5 shows th energy consumption of this case and figure 5.6 the absolute values of the consumed and regenerated energy.

Table 5.6: Comparing the results for Passauerhof-Maria Gugging with Nissan Leaf at 20 °C to 10 °C with fog

(a) 20 °C

γ/δ	0	0.2	0.4	0.6	0.8	1
0	(a)	(a)	(a)	(b)	(b)	(b)
0.2	(a)	(a)	**(a)**	(b)	(b)	-
0.4	(a)	(a)	(b)	(b)	-	-
0.6	(a)	**(a)**	(b)	-	-	-
0.8	**(a)**	(b)	-	-	-	-
1	(a)	-	-	-	-	-

(b) 10 °C with fog

γ/δ	0	0.2	0.4	0.6	0.8	1
0	(a)	(a)	(a)	(b)	(b)	(b)
0.2	(a)	(a)	**(b)**	(b)	(b)	-
0.4	(a)	(a)	(b)	(b)	-	-
0.6	(a)	**(b)**	(b)	-	-	-
0.8	**(b)**	(b)	-	-	-	-
1	(b)	-	-	-	-	-

5.3 Comparison of the Results

In order to compare the results from chapter 4 and chapter 5, they are shown in table 5.8. The table lists the trips at Wienerwald and San Francisco and gives the distances, the total elevation up and down, the energy consumption and the journey time. The time is only available for Wienerwald, because for San Francisco it would be too imprecise.

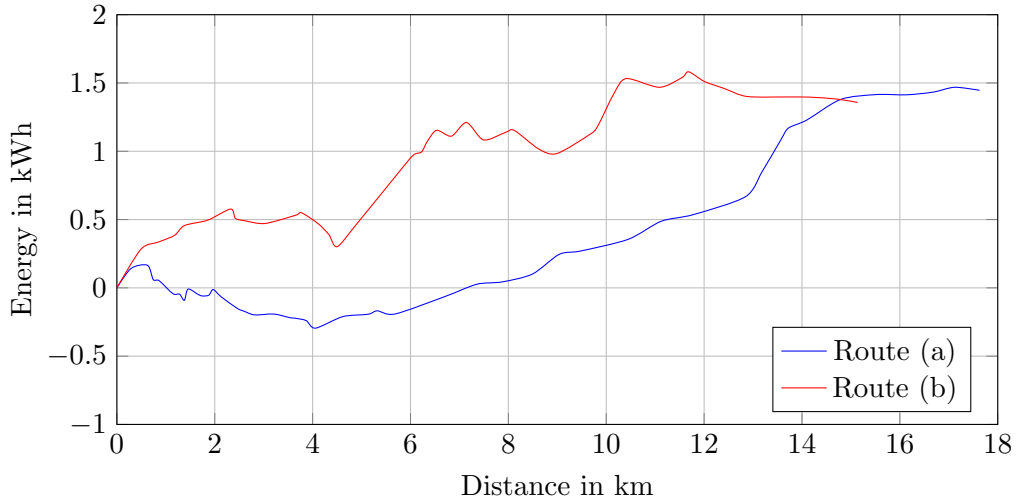

Figure 5.5: Energy consumption (cumulated) of route (a) and route (b) from Passauerhof to Maria Gugging

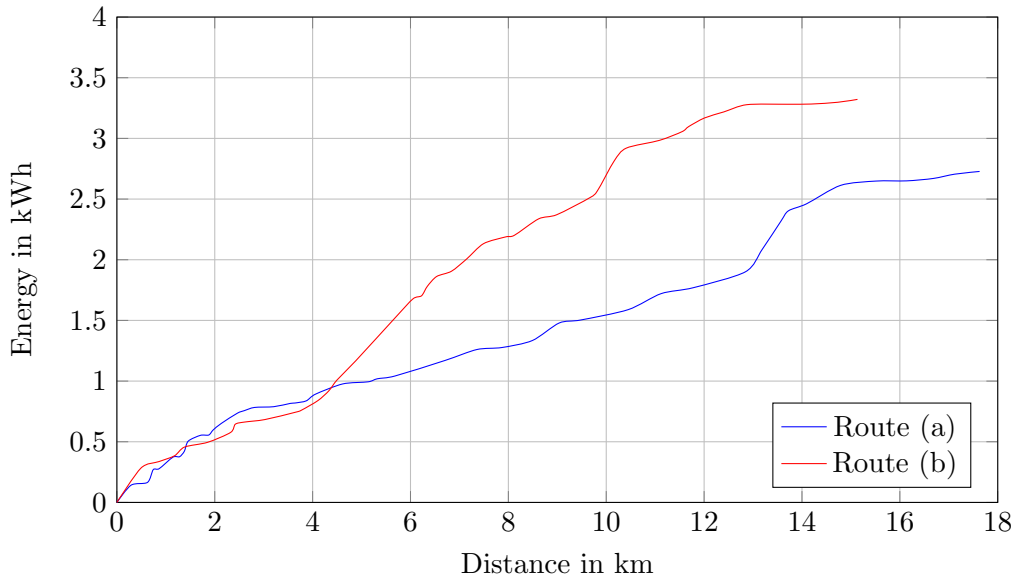

Figure 5.6: Absolute value (cumulated) of the energy consumed or regenerated of route (a) and route (b) from Passauerhof to Maria Gugging

Table 5.8: Comparison of different routes with different parameters

Route	Vehicle	Temp.	Distance	Up	Down	Energy	Time
Wienerwald							
Auhof - Sieghartskirchen (a)	Nissan	20 °C	20.47 km	211 m	231 m	2.19 kWh	22.68 min
Auhof - Sieghartskirchen (b)	Nissan	20 °C	29.68 km	383 m	403 m	4.81 kWh	22.45 min
Passauerhof - Maria Gugging (a)	Nissan	20 °C	17.63 km	122 m	299 m	1.02 kWh	19.70 min
Passauerhof - Maria Gugging (a)	Mitsubishi	20 °C	17.63 km	122 m	299 m	1.24 kWh	19.70 min
Passauerhof - Maria Gugging (a)	Nissan	−10 °C	17.63 km	122 m	299 m	2.03 kWh	19.70 min
Passauerhof - Maria Gugging (a)	Mitsubishi	−10 °C	17.63 km	122 m	299 m	2.15 kWh	19.70 min
Passauerhof - Maria Gugging (b)	Nissan	20 °C	15.13 km	203 m	380 m	1.04 kWh	16.06 min
Passauerhof - Maria Gugging (b)	Mitsubishi	20 °C	15.13 km	203 m	380 m	1.26 kWh	16.06 min
Passauerhof - Maria Gugging (b)	Nissan	−10 °C	15.13 km	203 m	380 m	1.85 kWh	16.06 min
Passauerhof - Maria Gugging (b)	Mitsubishi	−10 °C	15.13 km	203 m	380 m	1.95 kWh	16.06 min
San Francisco							
Pier 39 - Russian Hill	Nissan	20 °C	1.86 km	93 m	25 m	0.58 kWh	-
Russian Hill - Pier 39	Nissan	20 °C	1.86 km	24 m	92 m	−0.05 kWh	-
Union/Hyde - Lombard/Mason (a)	Nissan	20 °C	1.19 km	15 m	81 m	−0.12 kWh	-
Union/Hyde - Lombard/Mason (b)	Nissan	20 °C	0.90 km	15 m	79 m	−0.136 kWh	-
Union/Hyde - Lombard/Mason (c)	Nissan	20 °C	0.76 km	15 m	79 m	−0.139 kWh	-

6 Conclusion

The results of this thesis show that route planning specifically designed for electric vehicles has more to offer than conventional routing systems that find the shortest distance or the fastest path to a destination. Finding the most energy efficient path or a route that is best for the battery lifetime can increase the range and protect the battery.

The proposed route planning is tested for the Wienerwald area in Austria and for the city of San Francisco in California. The multi-objective optimization uses three optimization variables: energy consumption, journey time, and battery lifetime. With different weights on the variables, different solutions are obtained.

Analyzing real-world street networks, the results vary depending on the start and destination points. For some cases, there is only one optimal route for all variables. Other cases show very distinct results for one optimization variable.

The results in this work demonstrate the influence of the topography of the routes. The energy consumption depends significantly on the topography. Especially with electric vehicles, where energy can be regenerated by driving downhill, there is a strong correlation between energy consumption and topography.

Another aspect of this work is the optimization in order to increase the battery lifetime. Minimizing the total energy flow of the battery is the goal here and therefore routes with little variation of the topography are preferred. The battery is an expensive part of the vehicle and should be protected from degradation as much as possible.

The influence of the additional loads such as heating, air condition, lights, and fan is significant. Those loads are powered by the battery and therefore they increase the total energy consumption. An important factor is the duration of the journey, because the longer these additional loads operate, the more energy is used. Therefore, the results of the multi-objective optimization can change, because fast routes become more energy efficient.

It can be noticed that using a weighted multi-objective optimization is smarter than using a single-objective optimization. If the second best route in journey time is much more energy efficient, but only slightly slower, a time-only optimization would lead to an unreasonable result. Considering different aspects at the same time, the most convenient solution is achieved.

In order to use this type of route planning for real-world scenarios, some additional information would be necessary. First, traffic lights and stop signs should be included. Another important factor is traffic flow, because the optimal route can turn out to be a bad choice if the vehicle is stuck in traffic.

Future work on this topic should also include charging stations such that route planning is possible for trips longer than the range of the vehicle.

Another important aspect to be included in future work is driving behavior. Speed and acceleration influence the energy consumption of the vehicle. In urban areas, the journey time is mostly dependent on the traffic situation rather than speed, while in non-urban areas the speed can make a lot of difference. Assuming a certain speed profile would help achieving very realistic results. There could either be a statistical approach to obtain a speed profile or learning from previously obtained data of the driver's preferences.

List of Figures

List of Tables

Bibliography

Bellman, Richard (1958). "On a routing problem." In: *Quarterly of Applied Mathematics* 16, pp. 87–90 (cit. on pp. 5, 25).

De Nunzio, Giovanni and Laurent Thibault (2017). "Energy-optimal driving range prediction for electric vehicles." In: *2017 IEEE Intelligent Vehicles Symposium (IV)* (cit. on p. 6).

Dijkstra, E.W. (1959). "A note on two problems in connexion with graphs." In: *Numerische Mathematik 1*, pp. 269–271 (cit. on p. 5).

Geringer, Bernhard and Werner K. Tober (2012). *Batterieelektrische Fahrzeuge in der Praxis*. Tech. rep. Institut für Fahrzeugantriebe und Automobiltechnik, Technische Universität Wien (cit. on pp. 15, 33, 34, 44).

Haken, Karl-Ludwig (2013). *Grundlagen der Kraftfahrzeugtechnik*. Third edition. Carl Hanser Verlag München. ISBN: 978-3-446-43527-8 (cit. on pp. 10, 12, 13, 32).

Jeschke, Sebastian (2016). *Grundlegende Untersuchungen von Elektrofahrzeugen im Bezug auf Energieeffizienz und EMV mit einer skalierbaren Power-HiL-Umgebung*. Universität Duisburg-Essen (cit. on p. 16).

Mitsubishi (2018). URL: `https://www.mitsubishi-motors.com/en/showroom/i-miev/specifications` (visited on 04/03/2018) (cit. on p. 32).

Neaimeh, M. et al. (2013). "Routing systems to extend the driving range of electric vehicles." In: *IET Intelligent Transport Systems*. 3rd ser. 7 (cit. on p. 6).

Nissan (2018). URL: `https://www.nissan.co.uk` (visited on 03/19/2018).

Sachenbacher, Martin et al. (2011). "Efficient energy-optimal routing for electric vehicles." In: *25th AAAI Conference on Artificial Intelligence*, pp. 1402–1407 (cit. on p. 6).

Storandt, Sabine, Jochen Eisner, and Stefan Funke (2013). "Enabling e-mobility: One way, return, and with loading stations." In: *27th AAAI Conference on Artificial Intelligence* (cit. on pp. 6, 7).

Storandt, Sabine and Stefan Funke (2012). "Cruising with a battery-powered vehicle and not getting stranded." In: *26th AAAI Conference on Artificial Intelligence* (cit. on p. 6).

Yen, Jin Y. (1970). "An algorithm for finding shortest routes from all source nodes to a given destination in general networks." In: *Quarterly of Applied Mathematics* 27, pp. 526–530 (cit. on pp. 5, 26, 27).

Eidesstattliche Erklärung

Hiermit erkläre ich, dass die vorliegende Arbeit gemäß dem Code of Conduct – Regeln zur Sicherung guter wissenschaftlicher Praxis (in der aktuellen Fassung des jeweiligen Mitteilungsblattes der TU Wien), insbesondere ohne unzulässige Hilfe Dritter und ohne Benutzung anderer als der angegebenen Hilfsmittel, angefertigt wurde. Die aus anderen Quellen direkt oder indirekt übernommenen Daten und Konzepte sind unter Angabe der Quelle gekennzeichnet.

Die Arbeit wurde bisher weder im In– noch im Ausland in gleicher oder in ähnlicher Form in anderen Prüfungsverfahren vorgelegt.

Wien, 30. Mai 2018

Theresia Perger